Interplay of Aging Temperature and Thermophysical Properties of Lithium-Ion Battery Electrodes

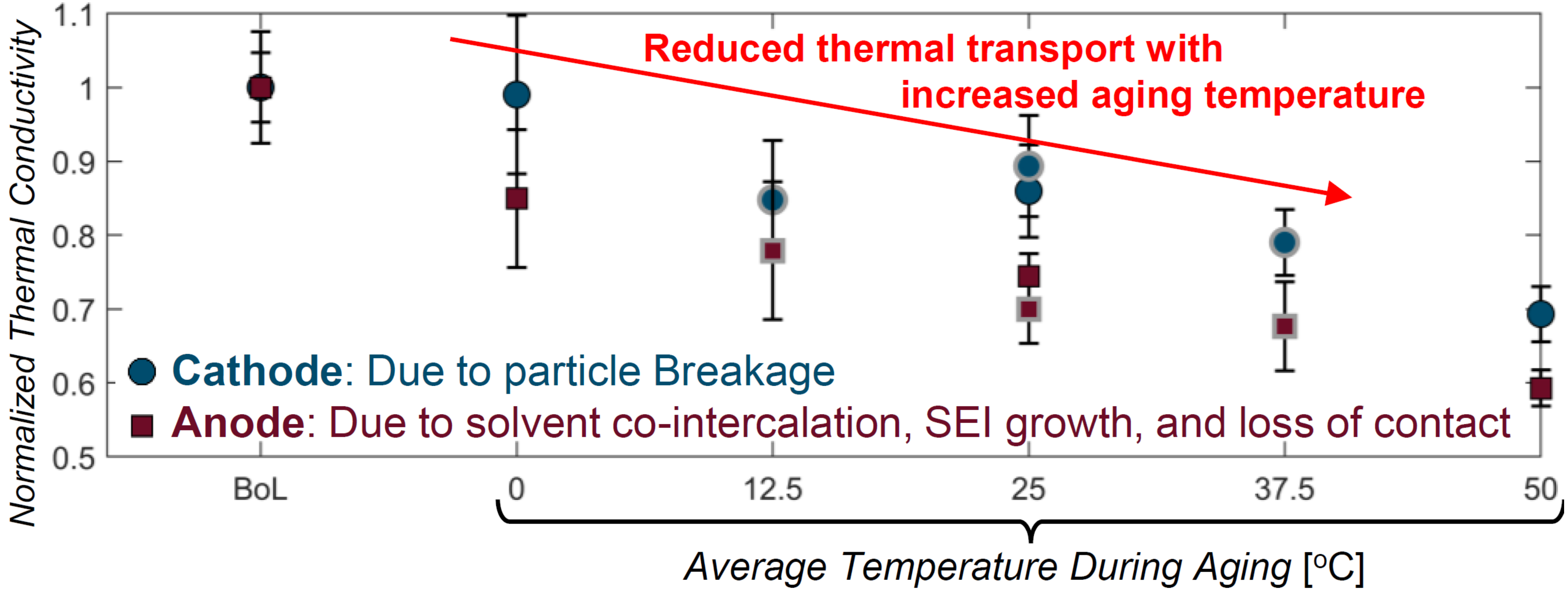

Unterstützt von / Supported by
Alexander von Humboldt Stiftung / Foundation
Karlsruher Institut für Technologie

Amy Marconnet (marconnet@purdue.edu)
S. Herberger, S. Paarmann, P. Seegert, and T. Wetzel
PURDUE UNIVERSITY
Mechanical Engineering

Motivation: Battery Safety & Reliability

Lithium battery in student backpack bla[...] Tahoe City hi[...]

Samsung factory fire caused by faulty batteries

'Minor' fire at Galaxy Note 7 battery supp[...] and 19 trucks sent to put out blaze, accor[...]

Apple looking into video of exploding iPhone 7 Plus

Apparent battery fire of rose gold iPhone 7 Plus prompts investigation following Samsung Galaxy Note 7 fears

Limited Data on Battery Thermal Properties

	Methodology	Electrode composition	Parameters	Anodes		Cathodes		Unit cell/Full cell	
				$k_\perp$ $Wm^{-1}K^{-1}$	$k_\parallel$ $Wm^{-1}K^{-1}$	$k_\perp$ $Wm^{-1}K^{-1}$	$k_\parallel$ $Wm^{-1}K^{-1}$	$k_\perp$ $Wm^{-1}K^{-1}$	$k_\parallel$ $Wm^{-1}K^{-1}$
Electrodes									
Maleki et al. [29]	XFT	$LiCoO_2$, Graphite	SOC, electrolyte	0.89–1.20	8.72–15.11	2.33–2.49	21.57–21.75	1.90–3.40	17.69–28.05
Nagpure et al. [30]	FT	$LiFePO_4$	Ageing effects	–	–	$2.0e^{-7}$–$3.8e^{-7}$ [a]	–	–	–
Burheim et al. [31]	CHF	$LiCoO_2$, Graphite	Composition, electrolyte	0.07(±0.01)–1.26(±0.07)	–	0.36(±0.03)–1.10(±0.06)	–	–	–
Full cells									
Murashko et al. [21]	CHF		SOC	–	–	–	–	0.59–0.74	–
Zhang et al. [22]	CHF	NMC/Graphite	–	–	–	–	–	0.48	21.00
Baszinski et al. [23]	CHF	$LiFePO_4$, NMC	SOC, T, composition	–	–	–	–	0.30–0.45	–
Fleckenstein et al. [24]	TIS	$LiFePO_4$/Graphite	–	–	–	–	–	0.35	–
Drake et al. [25]	Opened cell	$LiFePO_4$/Graphite	–	–	–	–	–	0.15–0.20[b]	30.4–32.0
Maleki et al. [28]	XFT	$LiCoO_2$/Graphite	Ageing effects	–	–	–	–	0.84–1.63	29.99–36.96

[a] Only thermal diffusivity given
[b] Radial thermal conductivity k_r of cylindrical cell

From Loges *et al.*. *J. Power Sources* 325, 104–115 (2016).

Generally Equivalent Properties Evaluated

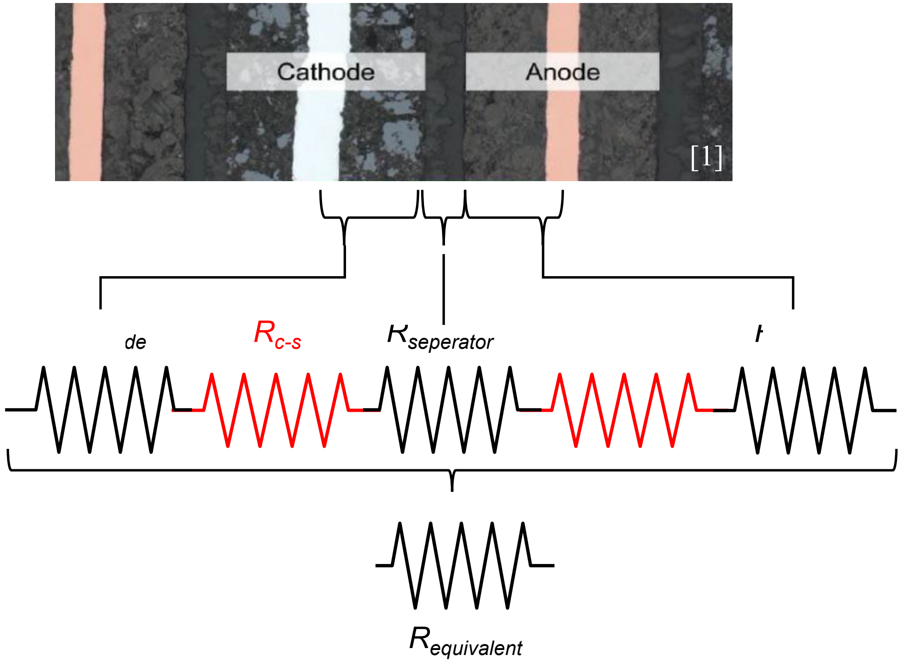

[1]Microscope image from AZoM

Objective & Project Organization

We propose to evaluate interfacial thermal contact resistances within lithium-ion batteries and their impact on battery performance and reliability.

Task 1: Battery Disassembly and Sample Preparation

- Sabine Paarmann's aging experiments provided a jump start on this
- Sabrina Herberger and a student, Benedikt Heider, prepared many of the samples, along with testing their density and heat capacity.

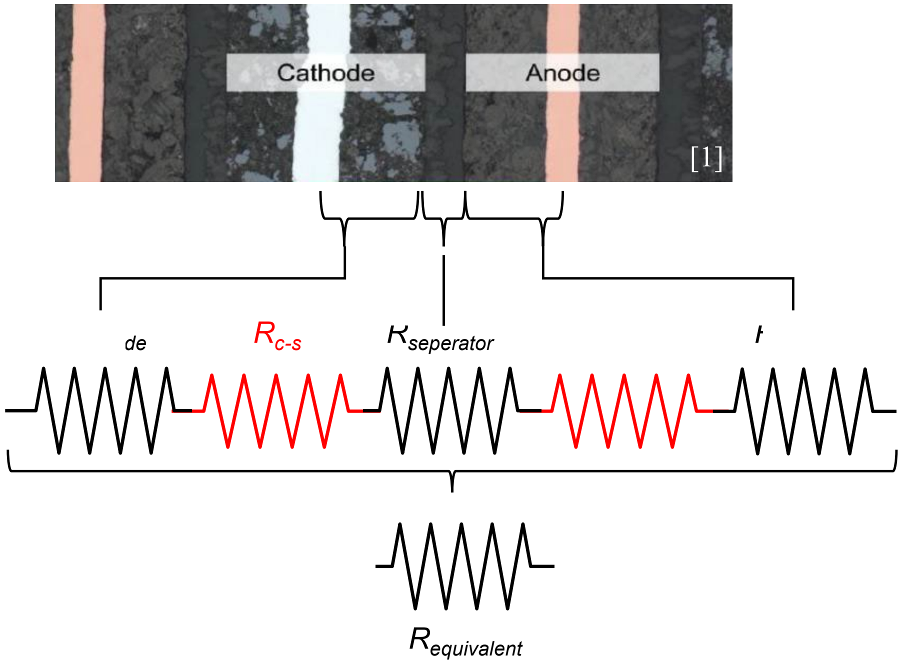

Task 2: Thermal Characterization

- Laser flash analysis (LFA) divided into 2 portions:
  - Conventional measurements of aged cell materials across a temperature range
  - Pressure cell for measuring multi-layer stacks at different pressure levels
    - Fully solid, well-known materials for analysis development
    - Battery materials
    - (Data analysis requires going beyond built-in models)

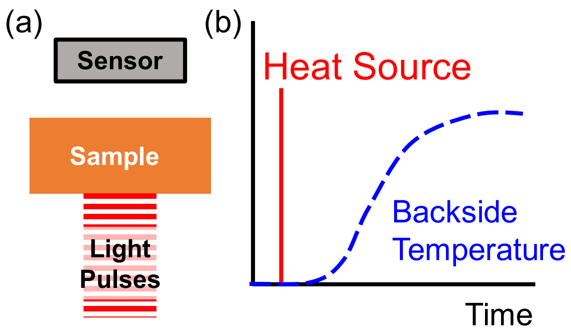

Task 3: Incorporating Thermal Resistances in Models

- Development of models for analyzing the LFA data
- Incorporation of resistances into models of battery cells will need more time

[1]Microscope image from AZoM

Thermal boundary conditions

Karlsruhe Institute of Technology

$T_0 = 0\ °C$; $T_1 = 25\ °C$; $T_2 = 50\ °C$

Inhomogeneous – Temperature gradient over the cell length
Transient – Temperature change with time

Stationary (S)

Transient (T)

Homogeneous (HS) | Inhomogeneous (IS) | Homogeneous (HT) | Inhomogenous (IT)

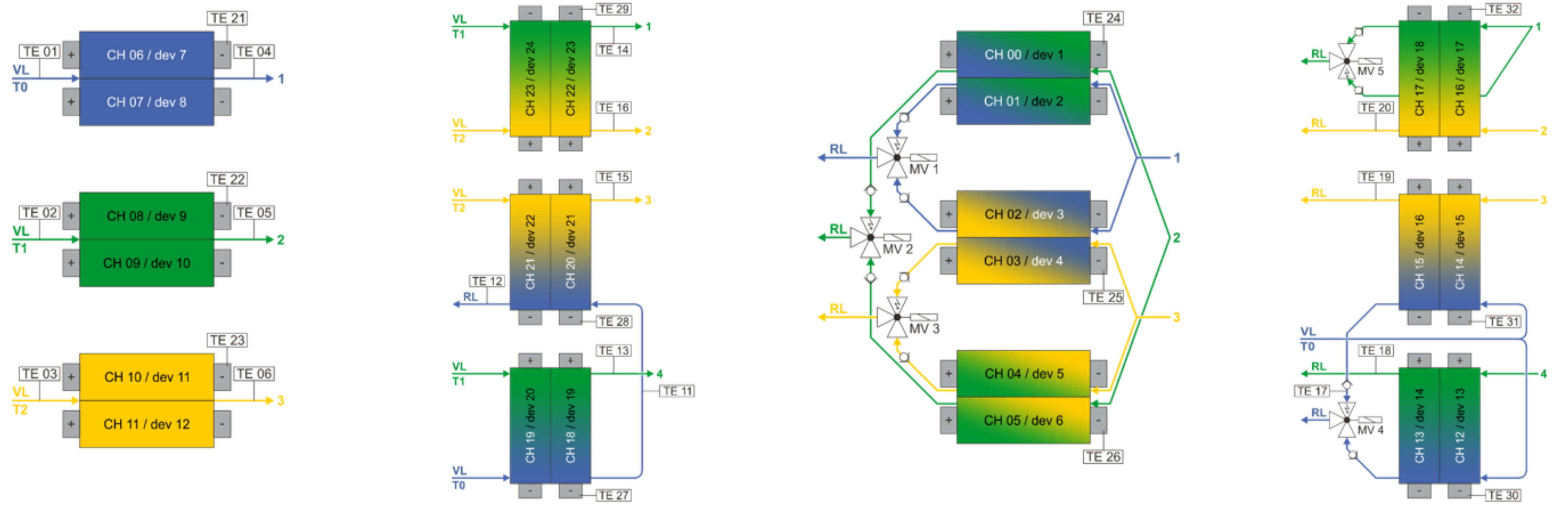

TVT Institute of Thermal Process Engineering

Sabrina's Data on Performance of Aged Cells

Sample ID	Aging Conditions	Average Aging Temperature [°C]	Equivalent Full Cycles
BoL	Beginning of Life (no aging)	N/A	N/A
HS0C	Homogeneous, stationary aging at 0°C	0	912
HS25C	Homogeneous, stationary aging at 25°C	25	8558
HS50C	Homogeneous, stationary aging at 50°C	50	8258
HT0-25C	Homogeneous, transient aging from 0 – 25°C	12.5	5239
HT0-50C	Homogeneous, transient aging from 0 – 50°C	25	5655
HT50-25C	Homogeneous, transient aging from 50 – 25°C	37.5	8024

➡ Temperature changes cause different behaviour than temperature gradients

Microstructural & Composition Changes with Aging

Post-mortem Analysis

Karlsruhe Institute of Technology

Temperature gradient 0 °C – 50 °C

Begin of Life

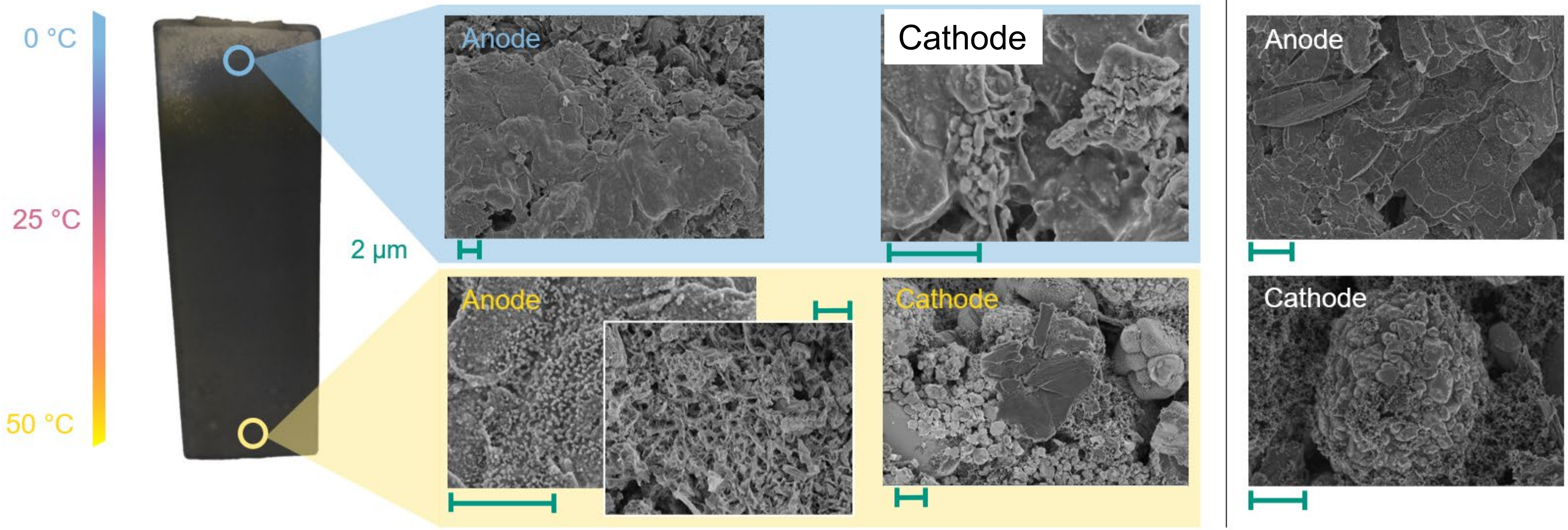

➡ Inhomogeneous ageing mechanisms occur according to local temperature

Preparing Aged Samples for Thermal Testing

Based on available materials and potential to quantify effect of aging, a subset of samples were selected for analysis:

- **Homogeneous Stationary:**
  - 0^{o}C
  - 25^{o}C
  - 50^{o}C
- **Homogeneous Instationary (Transient)**
  - 0^{o}C – 50^{o}C
  - 0^{o}C – 25^{o}C
  - 50^{o}C – 25^{o}C

Training by Julia Gandert
Sample preparation, DSC, and density measurements by Benedikt Heider and Sabrina Herberger

Analysis Techniques:

- DSC measurements of specific heat
- Pycnometry measurements to measure density
- LFA for thermal diffusivity
- Calipers for thickness

LFA Analysis Parameters:

- Three samples per aging test condition
- Two Gasses
  - Nitrogen (tested all 3 samples)
  - Hydrogen (tested 2 samples)
- -20^{o}C to 60^{o}C in 10^{o}C increments
- 3 laser shots per temperature step

Consider a pulse of heat at one surface of a slab, how long does it take for heat to diffuse to other surface?

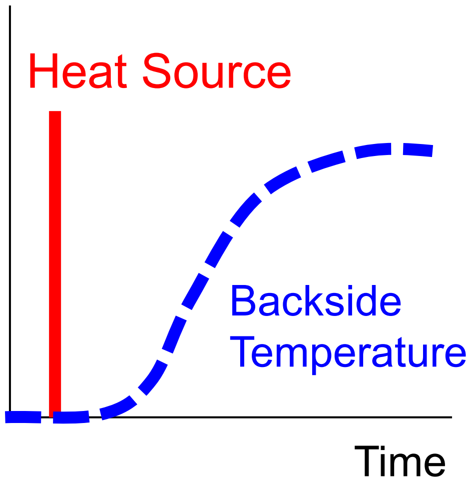

Heat Diffusion Equation (one dimensional):

$$\frac{\partial^2 T}{\partial x^2} = \frac{1}{\boxed{\alpha}} \frac{\partial T}{\partial t}$$

Thermal Diffusivity [m²/s] $\alpha = \frac{k}{\rho C_p}$

$$\frac{T}{L^2} \sim \frac{1}{\alpha}\frac{T}{t} \Rightarrow t \sim \frac{L^2}{\alpha}$$

→ The flash method is sensitive to the thermal diffusivity

What happens when sample consists of multiple sample sub-layers?

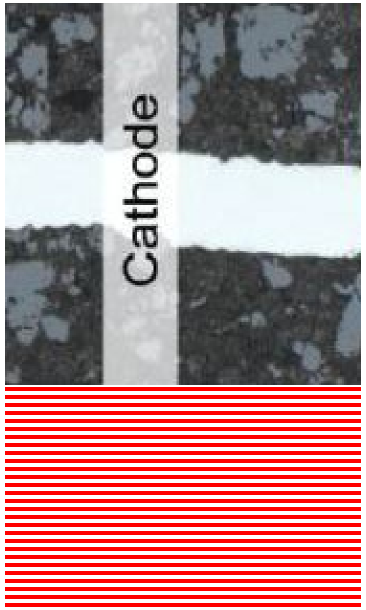

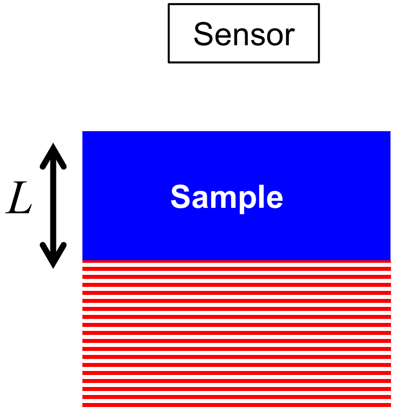

Flash Diffusivity

Image adapted rom http://www.azom.com/images/Article_Images/ImageForArticle_5813(2).jpg

Representative Data

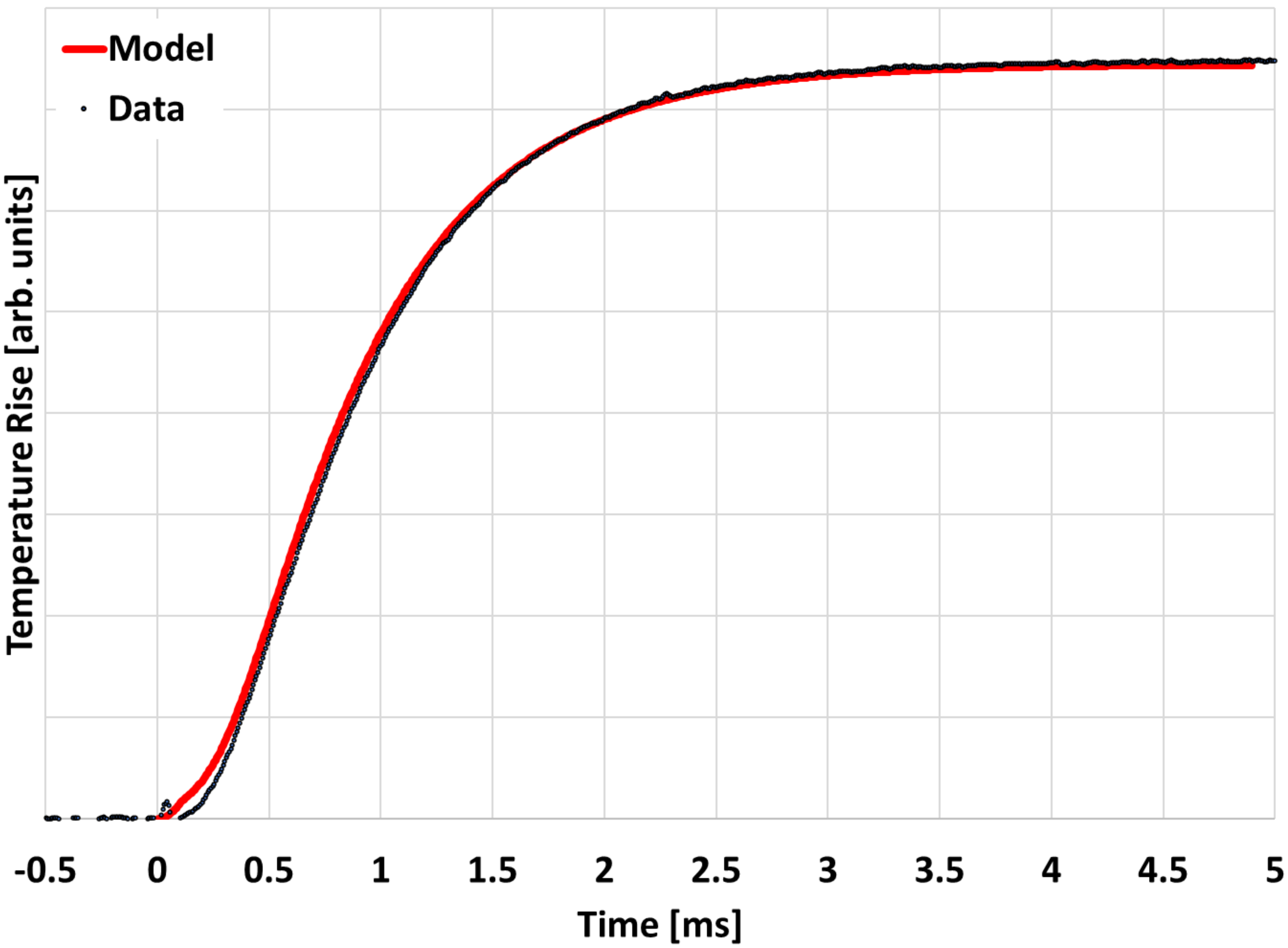

Measurement Parameters:

- For each aging condition, repeat multiple samples (extracted from different locations on the electrode).
- For each sample at each measurement temperature, average data from 3 "flashes"
- We generally used 3 samples for measurements in N2 atmosphere and 2 of those samples were measured in He atmosphere as well. Data is reported separately by atmosphere.
- For each data point on following slides, error bars are based in part on standard deviation of the samples combined with a detailed propagation of error analysis

Other Data Analysis Notes:

- Diffusivity fit data using built-in Netszch Software
- Model: Penetration + p.c.
- Time Range: 6 time constants

How do we get thermal conductivity from diffusivity?

For current collectors: Measure specific heat $C_{p,m}(T)$, density ρ_m, thickness d_m, and thermal conductivity $k_m(T)$ at BoL

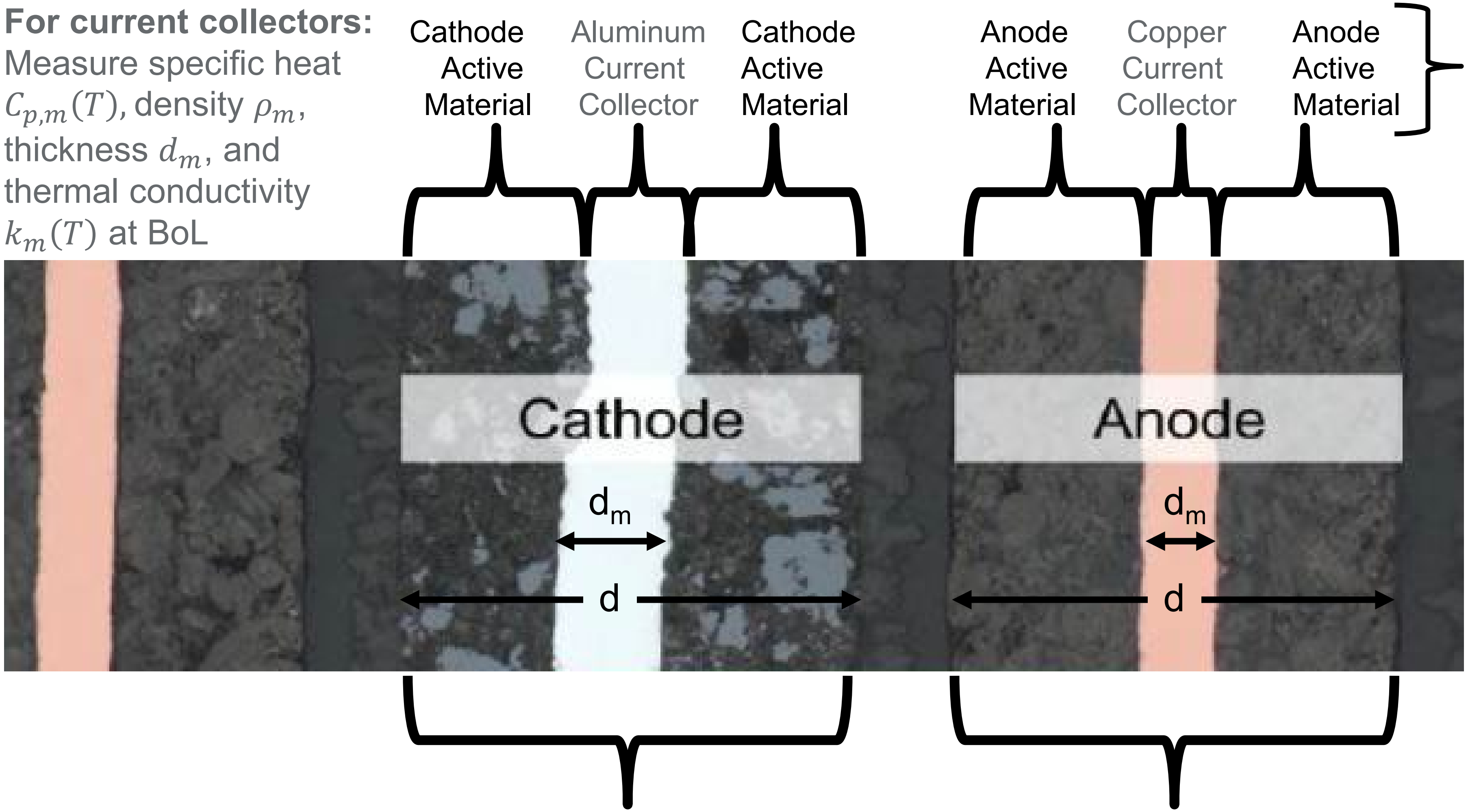

For active materials:

- Measure specific heat $C_p(T)$, density ρ, and porosity ϕ
- Calculate active material thickness $(d - d_m)/2$ and thermal conductivity $k_{active}(T)$ of the active material

- Porosity and metal properties are measured only at beginning of life
- Density and thickness are only measured at room temperature (23-25°C)
- Specific heat and thermal diffusivity are measured as functions of temperature

For each electrode:

- Measure thickness d and effective thermal diffusivity $\alpha(T)$ for the 3-layer stack
- Calculate thermal conductivity $k_{eff}(T)$ and volumetric heat capacity $\left(\rho C_p\right)_{eff}(T)$

Image adapted rom http://www.azom.com/images/Article_Images/ImageForArticle_5813(2).jpg

Estimating Thermal Conductivity

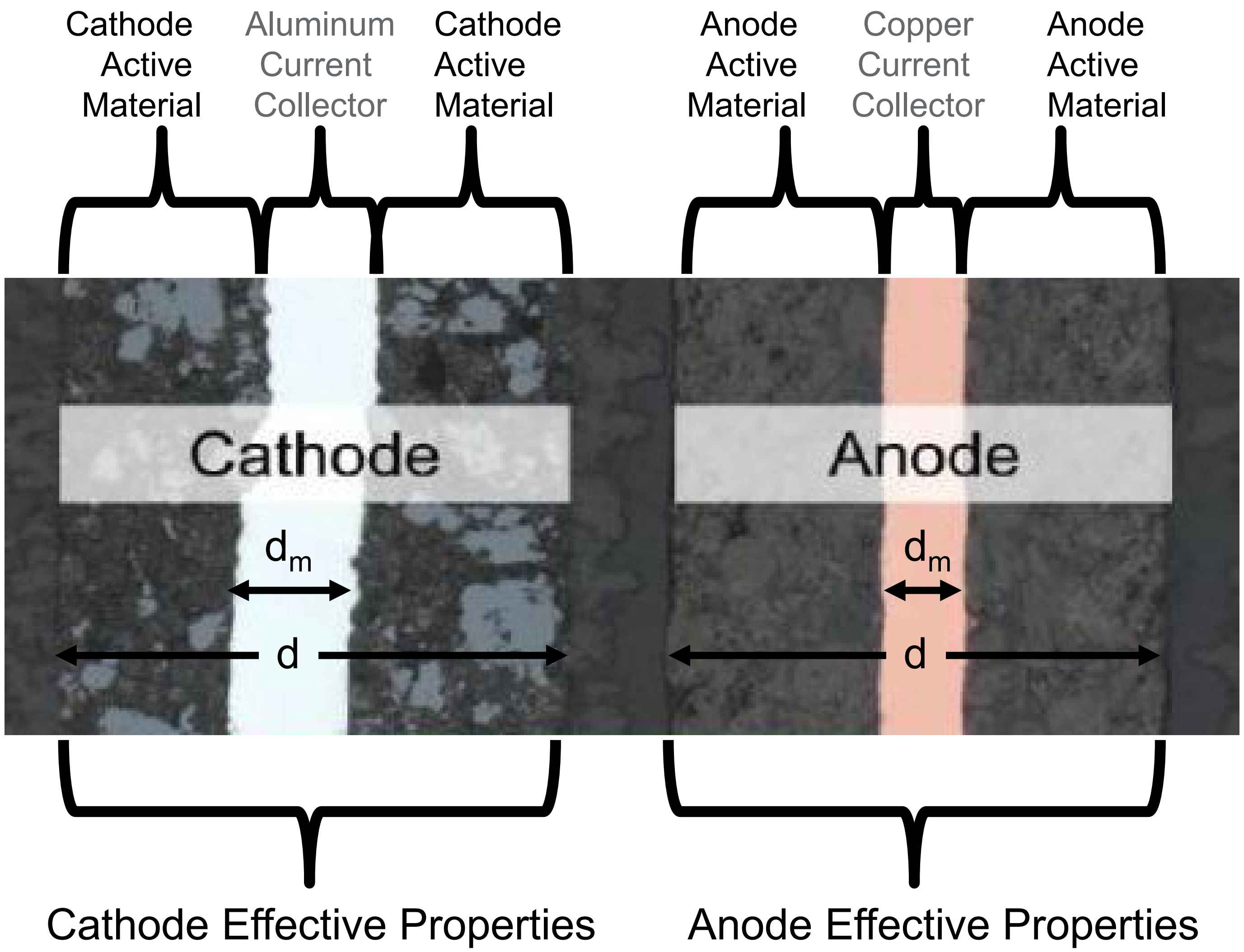

α_{eff} and $(\rho C_P)_{eff} \rightarrow k_{eff}$

Effective Thermal Conductivity:

$$\alpha_{eff} = \frac{k_{eff}}{(\rho C_P)_{eff}}$$

$$\boldsymbol{k_{eff} = \alpha_{eff}(\rho C_P)_{eff}}$$

Thermal Conductivity of the Active Material :

$$R_{th,eff} = \frac{d}{k_{eff}} = \frac{2d_{act}}{k_{active}} + \frac{d_m}{k_{metal}}$$

$$\boldsymbol{k_{act} = \frac{d - d_m}{\frac{d}{k_{eff}} - \frac{d_m}{k_m}}}$$

Image adapted rom http://www.azom.com/images/Article_Images/ImageForArticle_5813(2).jpg

Sensitivity / Uncertainty Analysis

Representative data shown for the BoL sample measured at 20°C

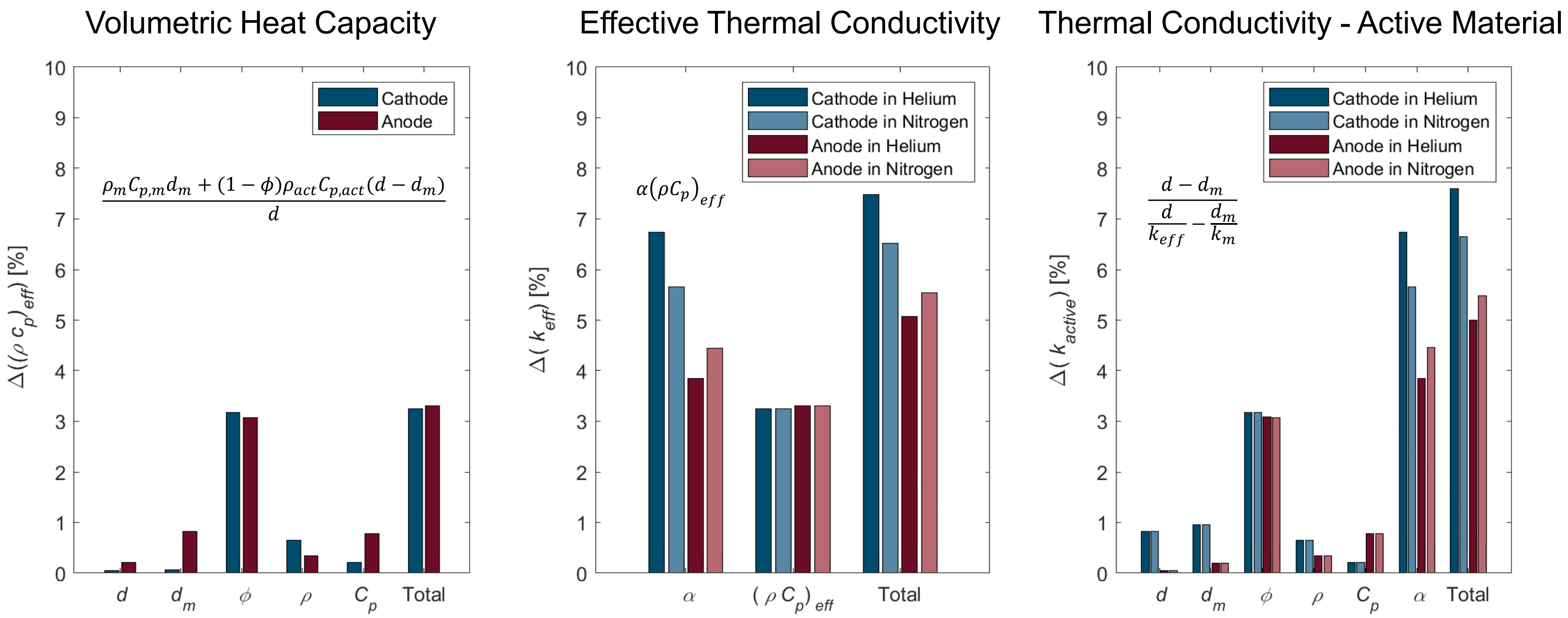

$$\Delta M = \sqrt{\sum_j \left(\frac{\partial M}{\partial x_j}\Delta x_j\right)^2}$$

Normalized Uncertainty in the Measured Parameter

Parameter	Range	BoL Sample Measured at 20°C	Uncertainty Causes
d	0.7 – 4.4 %	1.2% (Anode); 2.8% (Cathode)	Sample-to-sample and spot-to-spot variation
d_m	3.0-3.1%	3.0% (Anode); 3.1% (Cathode)	Sample-to-sample and spot-to-spot variation
ϕ	10%	10%	Sample-to-sample variation; Different measurement types
ρ	0.5 – 1.3%	0.5% (Anode); 0.9% (Cathode)	Sample-to-sample variation
C_p	0.3 – 3.2 %	1.1% (Anode); 0.3% (Cathode)	Sample-to-sample variation
α	0.3 – 11%	2.9% (Anode) ; 4.1% (Cathode)	Sample-to-sample variation
	1.6 – 11%	2.6% (Anode); 5.3% (Cathode)	Uncertainty in thickness impacting uncertainty in fitted α

Impact of Measured Thickness on Thermal Diffusivity

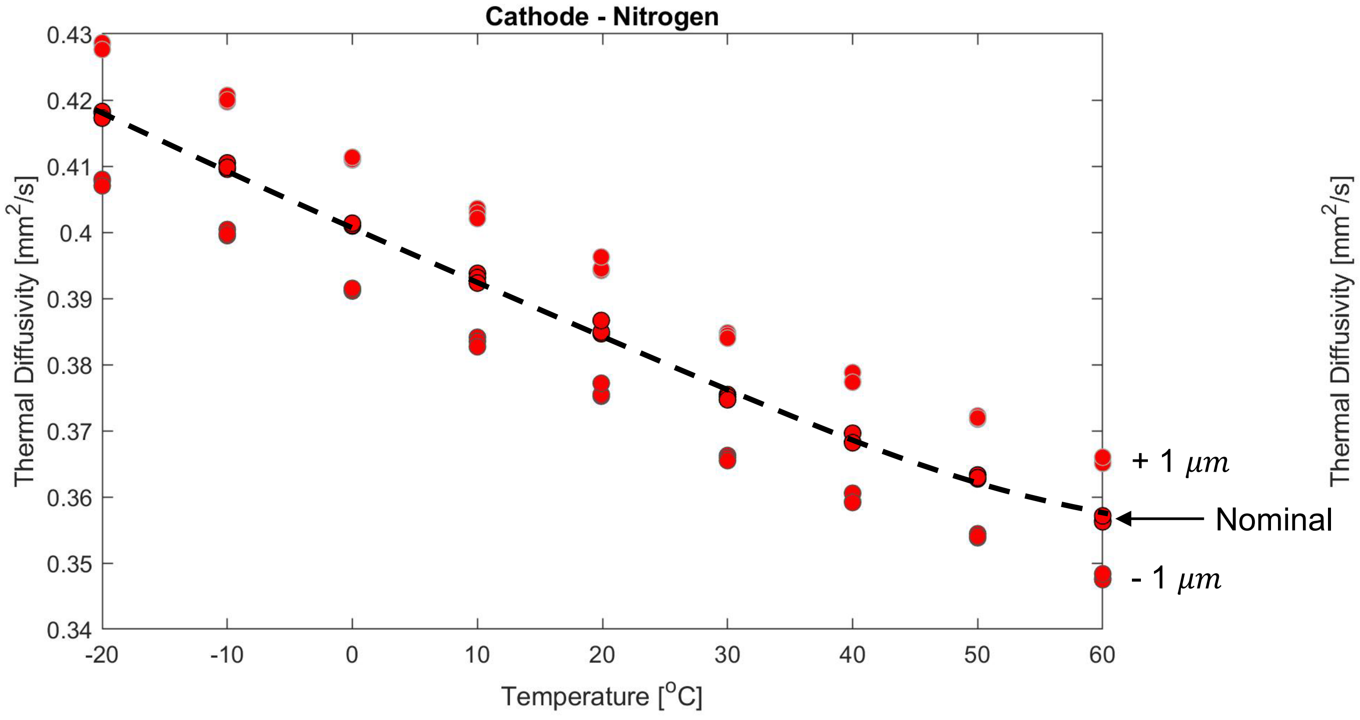

Approximately +/- 0.01 mm²/s or 2.5% per μm uncertainty

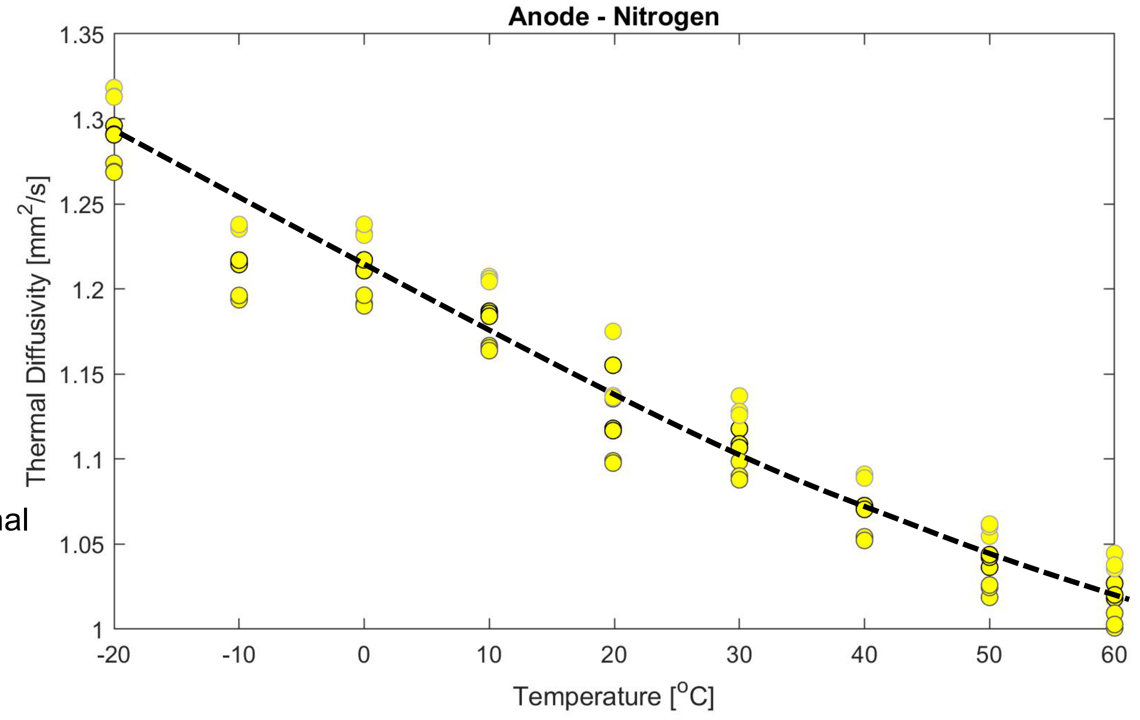

Approximately +/- 0.02 mm²/s or 2% per μm

Aging Conditions	Input Thickness		
	- 1 μm	Nominal	+1 μm
HS 50°C	●	●	●
HI 0-50°C	●	●	●

In addition to impacting the fit for effective diffusivity, the thickness impacts the extraction of the active material thermal conductivity:

$$k_{act} = \frac{d - d_m}{\frac{d}{k_{eff}} - \frac{d_m}{k_m}}$$

Measured sample-to-sample thickness variation: 1 – 5 μm

Trends for Electrode Thermal Diffusivity

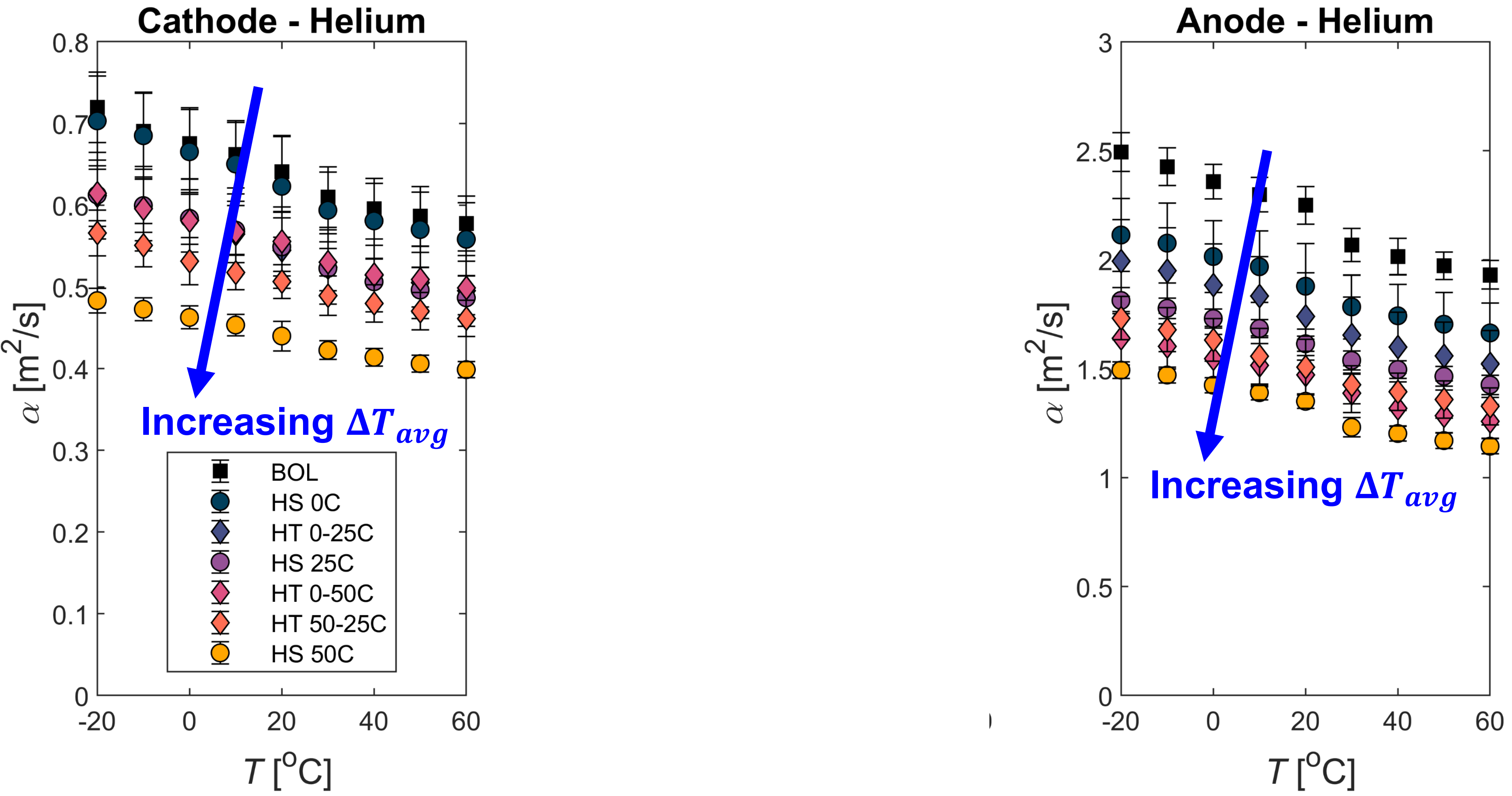

- Thermal diffusivity of anode (copper & graphite) is greater than that of cathode (NCA/LCO & aluminum)
- Effective thermal diffusivity decreases with increasing measurement temperature
- Effective thermal diffusivity decreases with increasing average aging temperature
- Measurements in helium generally larger than those in nitrogen

Effective Volumetric Heat Capacity

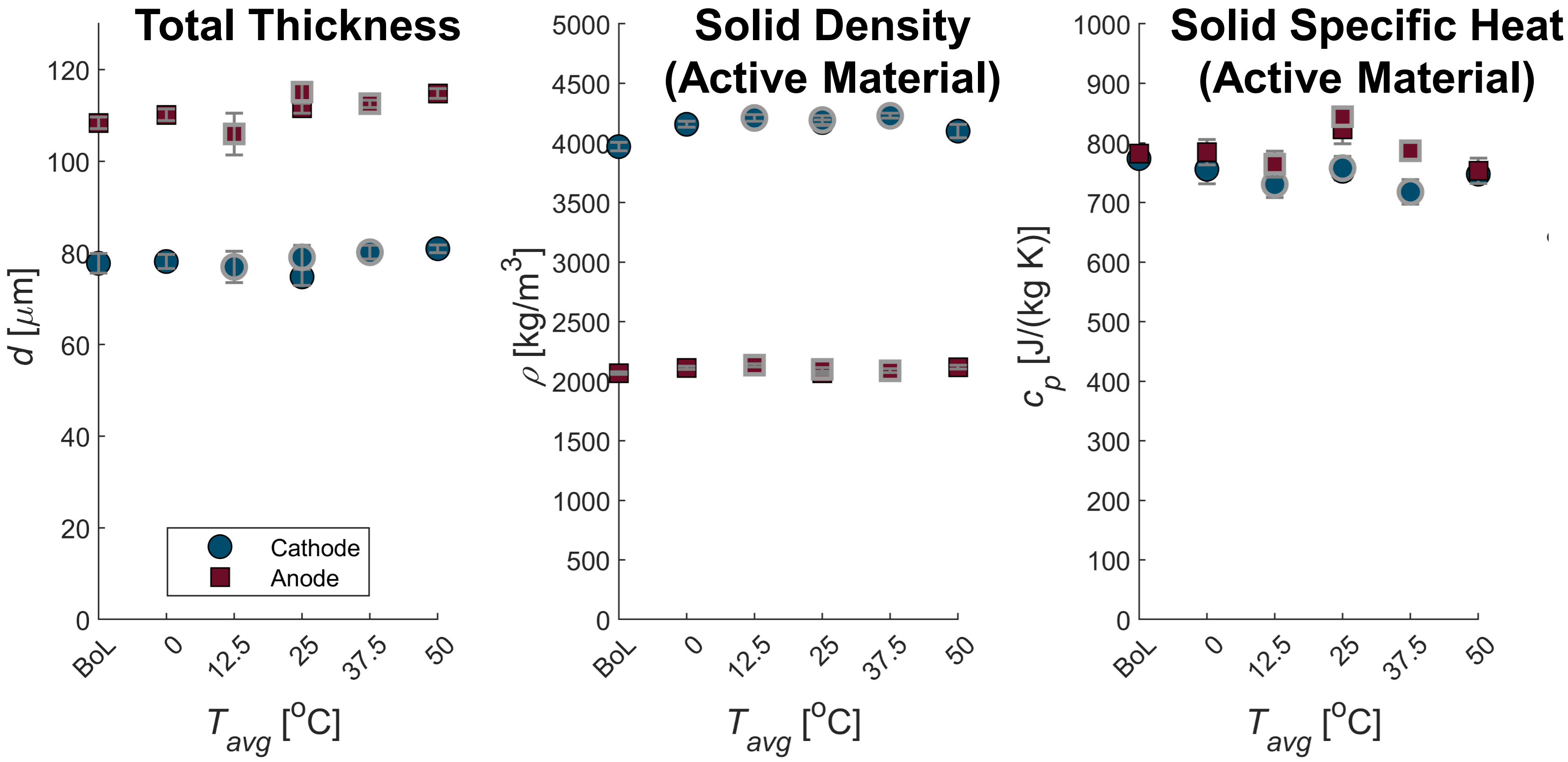

Measure:

- d (total thickness of electrode)
- ρ and C_p of the solid active material with aging
- d_m, ρ_m, and $C_{p,m}$ of the solid metal layer at BoL
- ϕ (porosity) of the active electrode layer at BoL

Calculate:

$$(\rho C_p)_{eff} = \frac{\rho_m C_{p,m} d_m + (1-\phi)\rho_{act} C_{p,act}(d - d_m)}{d}$$

Volumetric heat capacity relatively insensitive to aging conditions

Effective Thermal Conductivity

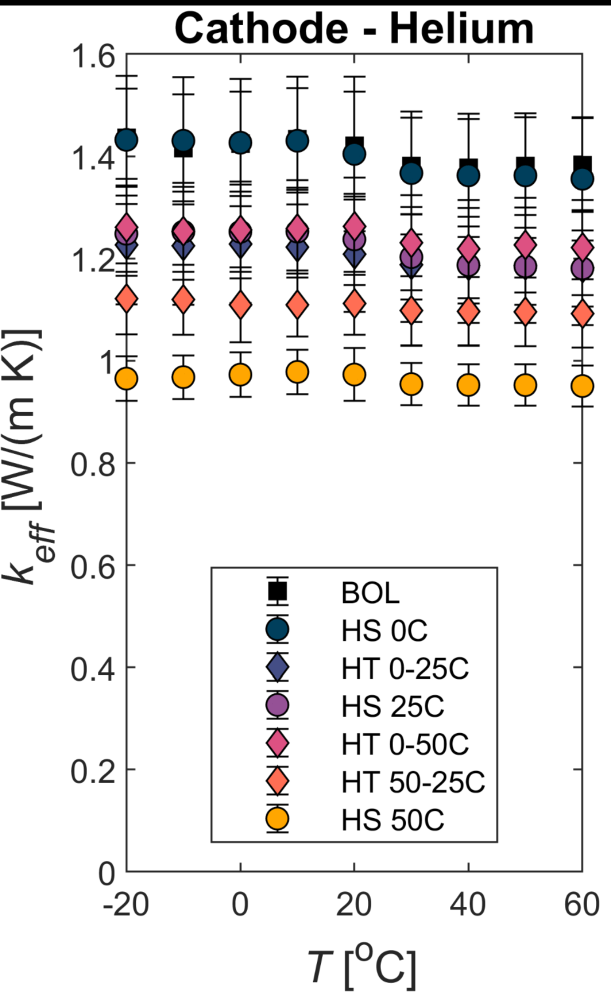

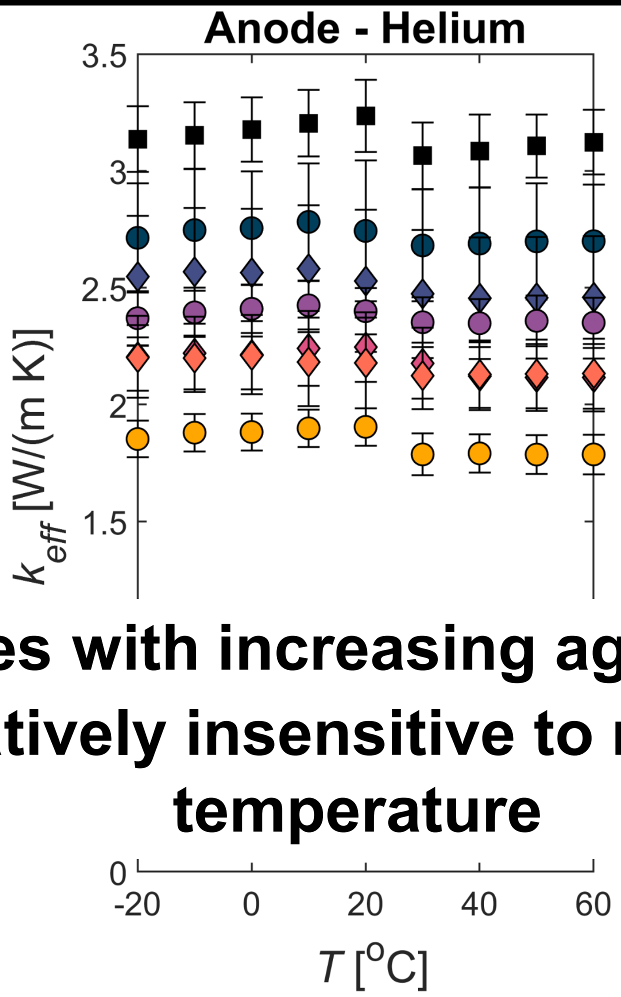

k_{eff} decreases with increasing aging temperature and is relatively insensitive to measurement temperature

Measure: α of the 3-layer electrode stack (active-metal-active)

Calculate: $k_{eff} = \alpha(\rho C_p)_{eff}$

Measure Sub-Components and Calculate: $(\rho C_p)_{eff}$

Estimate Active Material Thermal Conductivity

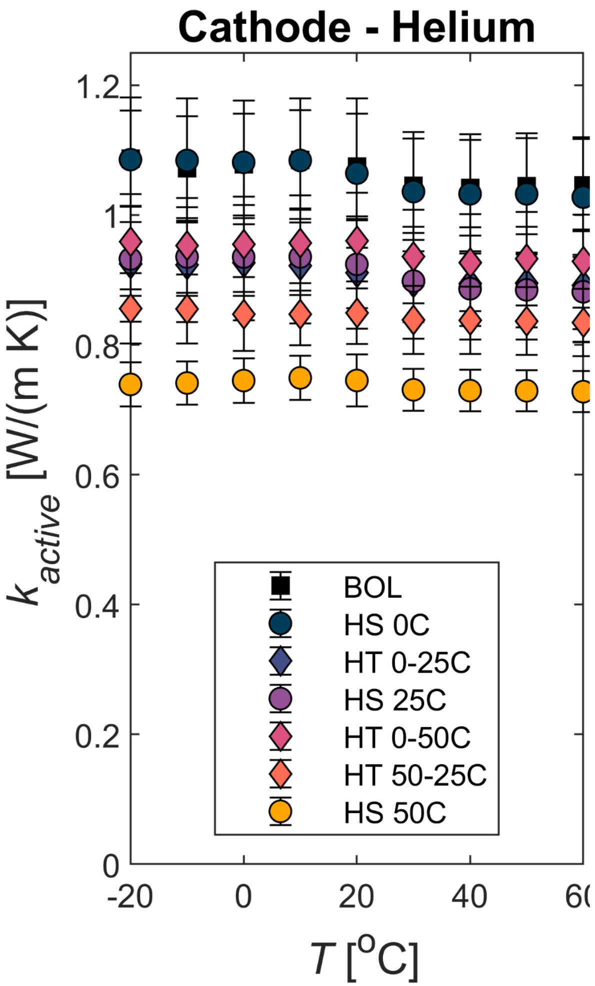

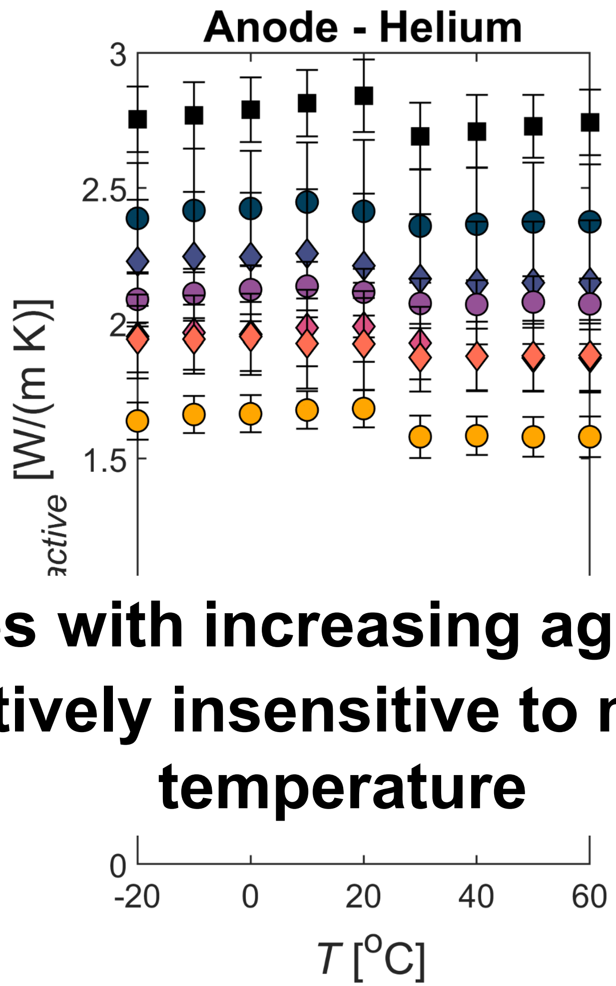

k_{eff} decreases with increasing aging temperature and is relatively insensitive to measurement temperature

Measure: α of the 3-layer electrode stack (active-metal-active), d, d_m, and k_m

Measure Sub-Components and Calculate: $(\rho C_p)_{eff}$,

Calculate: $$k_{act} = \frac{d - d_m}{\frac{d}{k_{eff}} - \frac{d_m}{k_m}}$$

Normalized Results with Average Aging Temperature

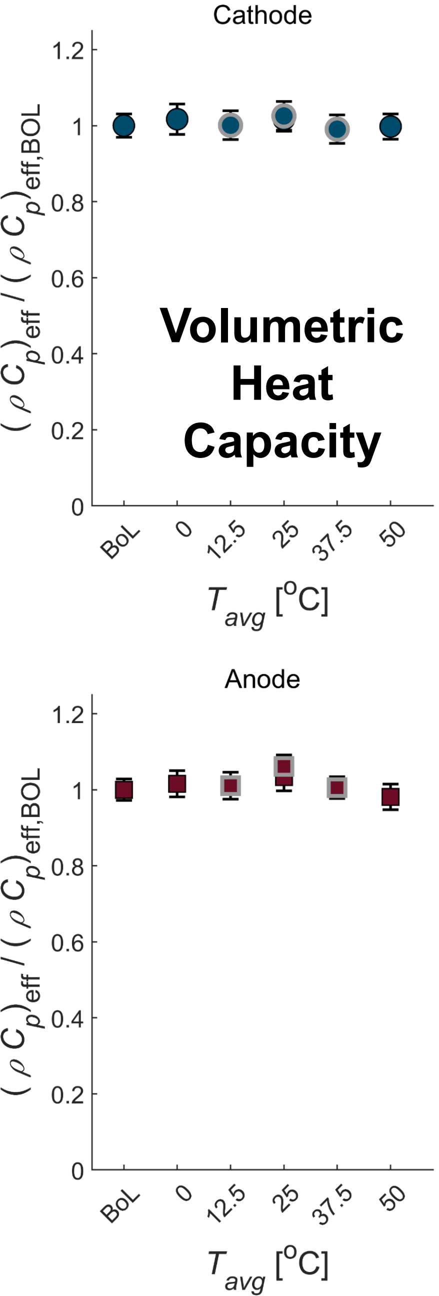

Clear decrease in effectiveness of thermal transport with higher aging temperatures.

Why is thermal transport impacted by aging?

Proposed Explanation: Mechanical Structure Evolution

5 Non-Uniform Tempe

Increasing diffusivity

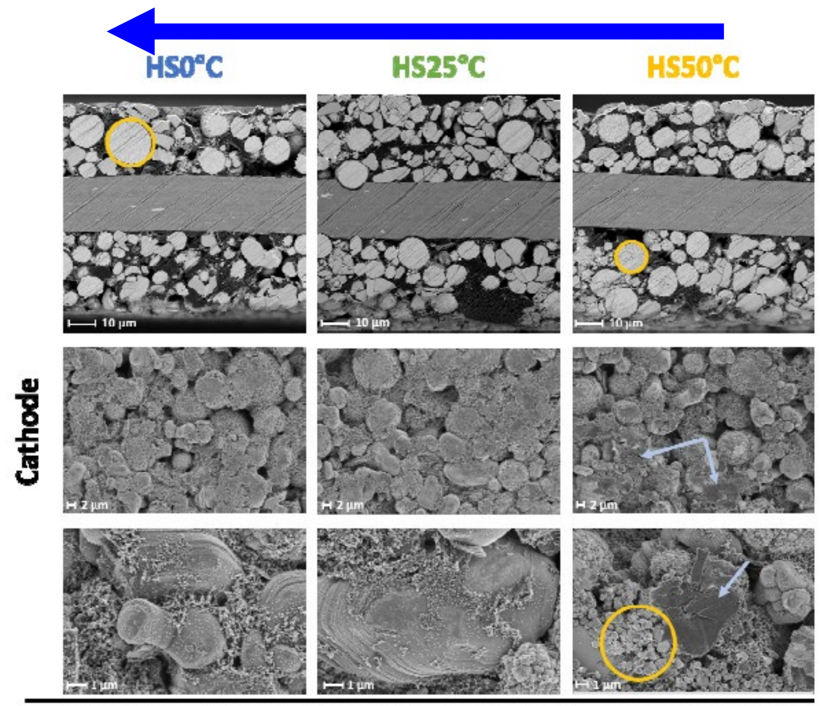

Figure 32. SEM images at EoL of cathode cross-section (first row) and surface (second and third row) and the anode surface (fourth and fifth row) for cycling at homogeneous stationary temperature control at 0 °C (first column), 25 °C (second column), and 50 °C (third column).

Cathode: Particles Cracking

SEM images of cross-sections and surfaces in Figure 32 show detailed changes for the different thermal conditions. Primary particles of NCA increasingly lose their adhesion at elevated temperature resulting in reduced integrity and finally cracking of secondary particles along the boundaries between the primary particles. This is visible in the cross-sections of the cathode for the HS boundary condition in Figure 32, indicated by yellow circles. After cycling at 0 °C, the primary particles composing the secondary particles are not discernible, just as in the BoL state. The first secondary particles break during cycling at 25 °C, and at 50 °C, the primary particles of each secondary particle are well identifiable, and some are completely broken. This is also evident in the close up of the surface circled in yellow. The particle rupture probably is a consequence of higher mechanical stress caused by phase transformation. At elevated temperatures, the cut-off voltages are reached after a larger charge throughput, and the phase transformation, which occurs mainly at high voltages [290], is completely undergone. Whether the same is valid for LCO can not be revealed by the electrode sections analysed. Furthermore, in the surface images, there are more deposits visible for increasing cycling temperature. The cathode that was cycled at 50 °C shows darker patches which seem to be flake-like particles (blue arrows). The graphite anode does not exhibit any alteration in the cross-section, so the images are not shown.

Figure and text from Sabine Paarmann's dissertation
https://publikationen.bibliothek.kit.edu/1000139983

Proposed Explanation: Mechanical Structure Evolution

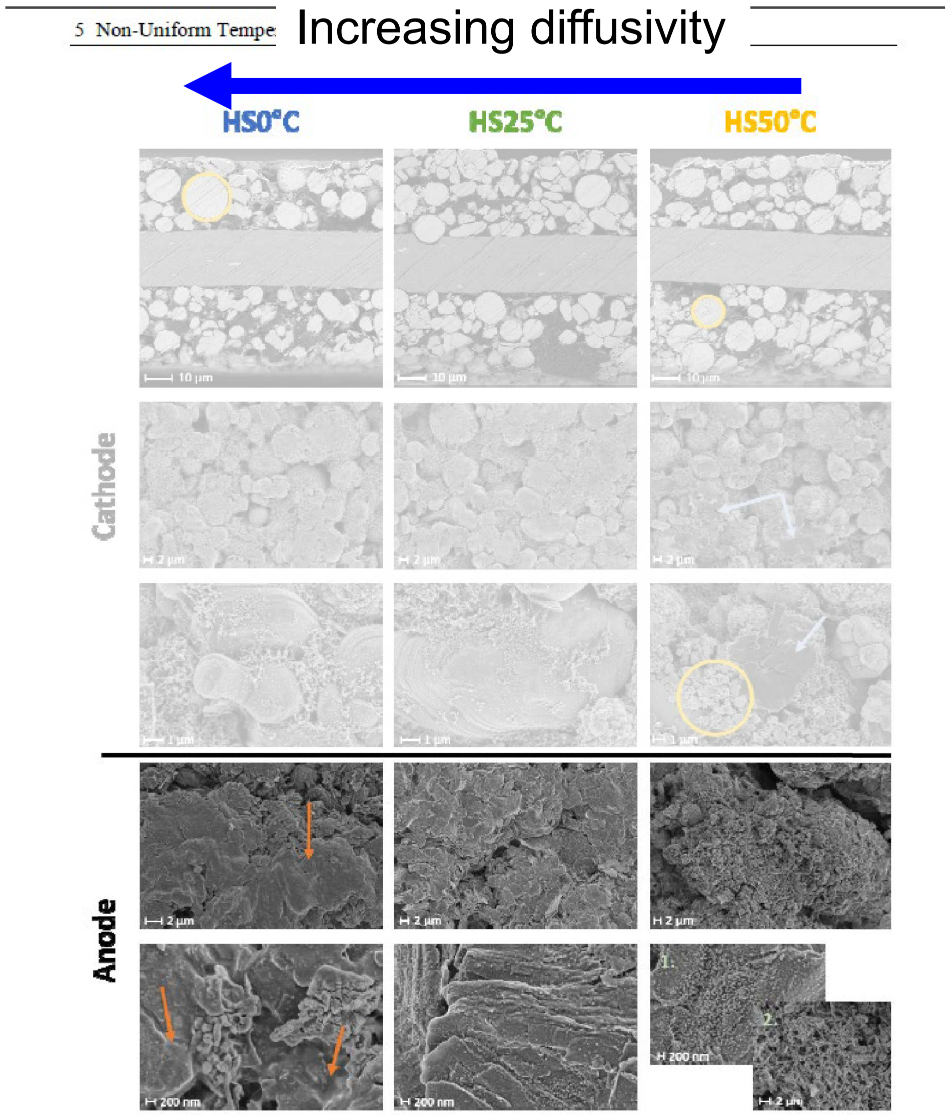

Figure 32. SEM images at EoL of cathode cross-section (first row) and surface (second and third row) and the anode surface (fourth and fifth row) for cycling at homogeneous stationary temperature control at 0 °C (first column), 25 °C (second column), and 50 °C (third column).

Anode: Explanation less obvious

- Dr. Paarmann's dissertation identified evolution of lithium morphology

  However, the inspection of the surface reveals significant modifications. The anode cycled at 0 °C is, in some places, coated with a thick homogeneous layer that looks like it is shrunk on the surface (orange arrows) and is assumed to be one morphology of plated lithium. Otherwise, there is little change in the typical flake structure of graphite in this case. For 25 °C, there are minor changes compared to BoL as the surface layer, probably SEI, blurs the edges of the flakes slightly more. The anode cycled at 50 °C exhibits much more non-uniform surface phenomena. Again, the blurring of the edges is visible together with tiny granular deposits in the first picture attributed to electrolyte degradation and SEI, while in other regions and the second picture, clusters of needle-like crystals appear. Presumably, this constitutes another morphology of lithium plating. These findings suggest that the morphology of plated lithium depends on the cycling temperature. While the deposits tend to be needle-like or granular at high temperatures, they are more planar and homogeneous at low temperatures. This observation is supported by Park et al. [291], who report less dendritic growth for lower temperature and Li et al., who state that for extensive deposition, the morphology is planar [200].

- Additionally, solvent co-intercalation and exfoliation separate the layers of carbon atoms within the graphite, potentially reducing the particle thermal conductivity,
- Furthermore, the growth of the SEI and loss of contact may increase the thermal contact resistances between graphite particles.

Figure and text from Sabine Paarmann's dissertation
https://publikationen.bibliothek.kit.edu/1000139983

How can overcome metrology limitations of laser flash?

Challenges with Laser Flash:

- Laser flash measures effective diffusivity of 3-layer electrode stacks
  (requires self-supporting sample)
- Real battery electrodes are infiltrated with an electrolyte that impacts properties
- Real battery cells operate with some pressure compressing the layers

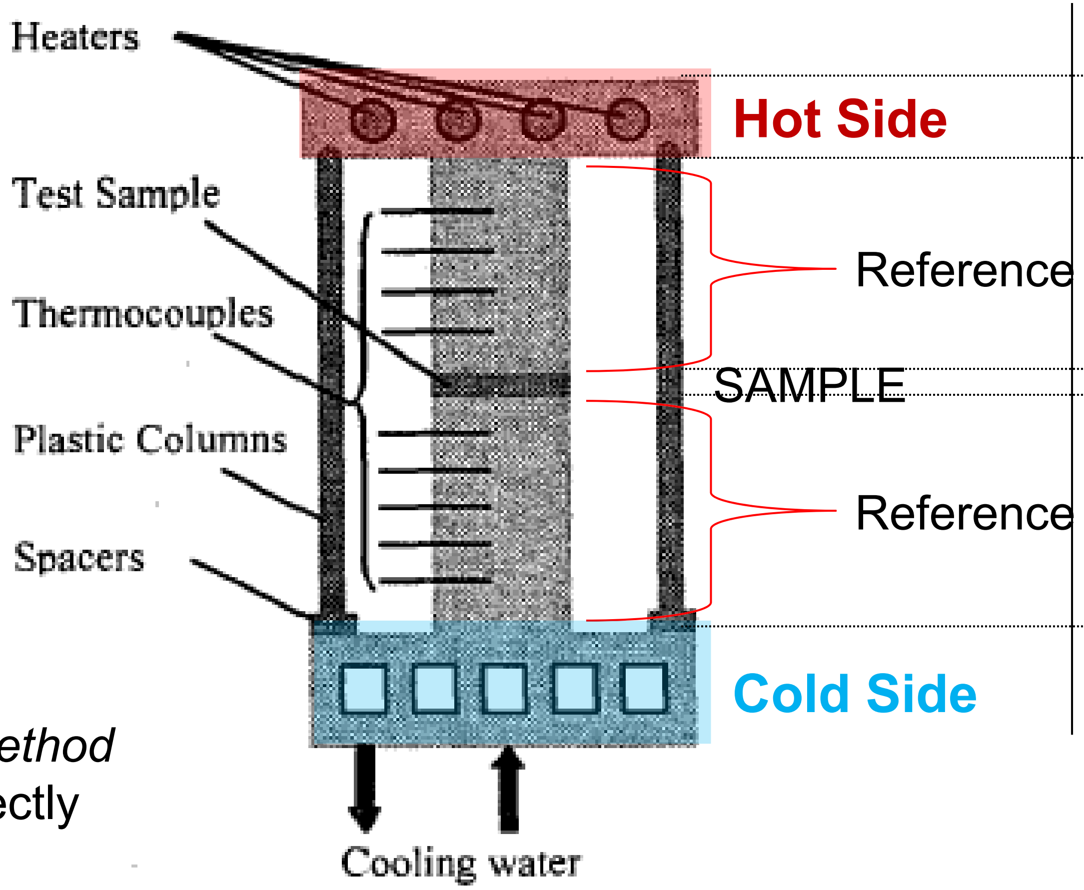

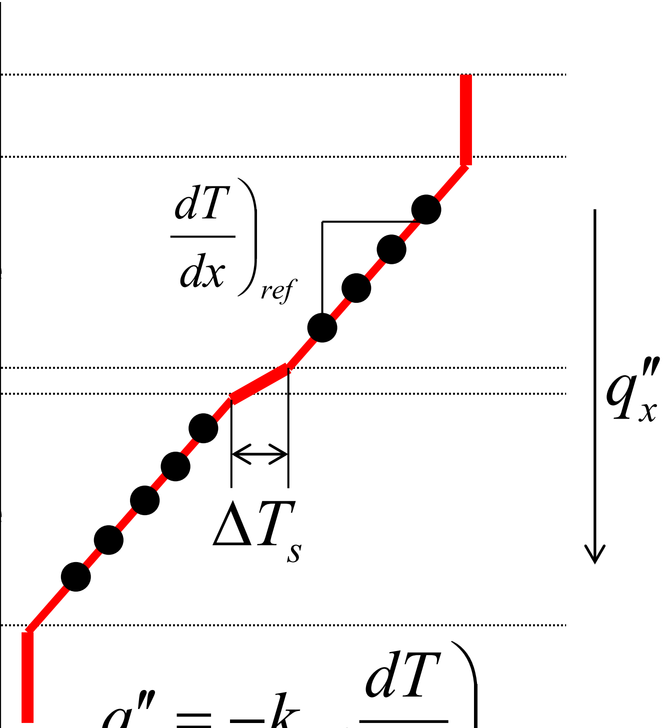

$$q''_x = -k_{ref} \left.\frac{dT}{dx}\right)_{ref}$$

Potential Resolution:

Infrared-Enhanced Reference Bar Method

- Steady state measurement → directly resolve thermal conductivity
- Repeat measurements with varying pressure across the sample
- Infrared imaging to potentially resolve thermal properties of individual layers
- Electrolyte??

$$q_x = G_{th,s}\Delta T_s = \frac{k_s A}{L_s}\Delta T_s \rightarrow k_s = q''_x L_s / \Delta T_s$$

X. Hu, *et al.*, "Thermal conductance enhancement of particle-filled thermal interface materials using carbon nanotube inclusions," in *The Ninth Intersociety Conference on Thermal and Thermomechanical Phenomena in Electronic Systems (ITHERM '04)*, 2004, pp. 63-69 Vol.1.

Miniaturized Reference Bar Method

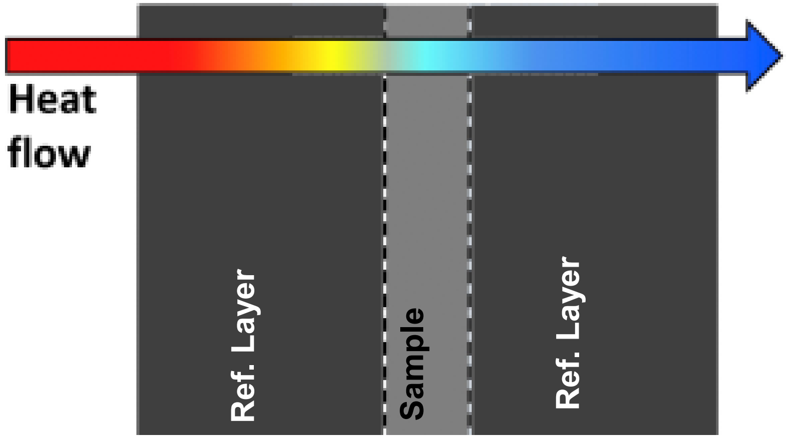

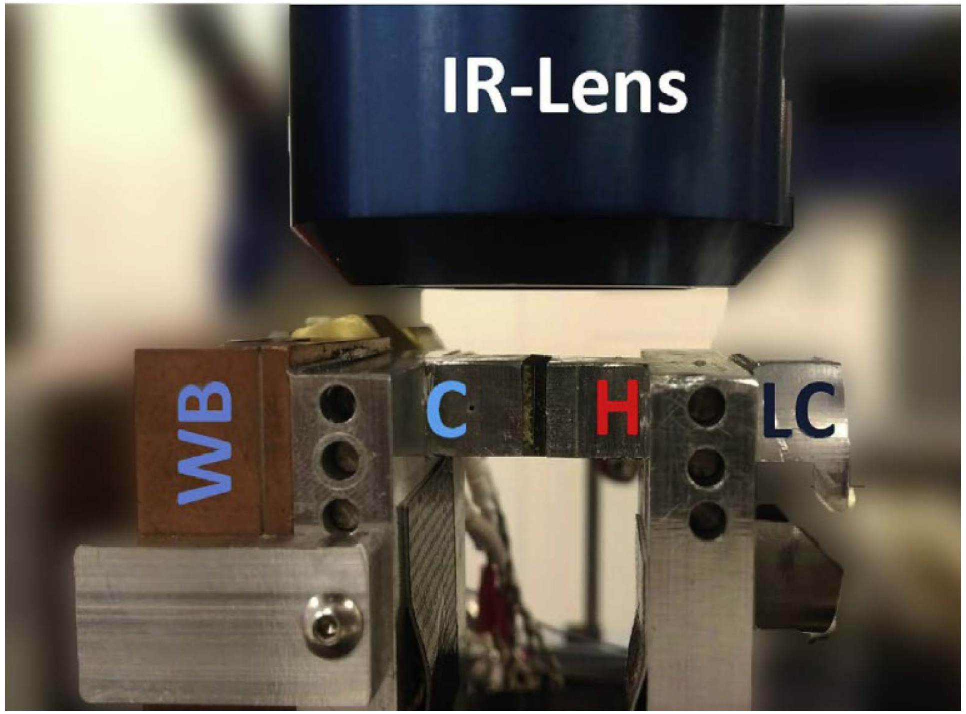

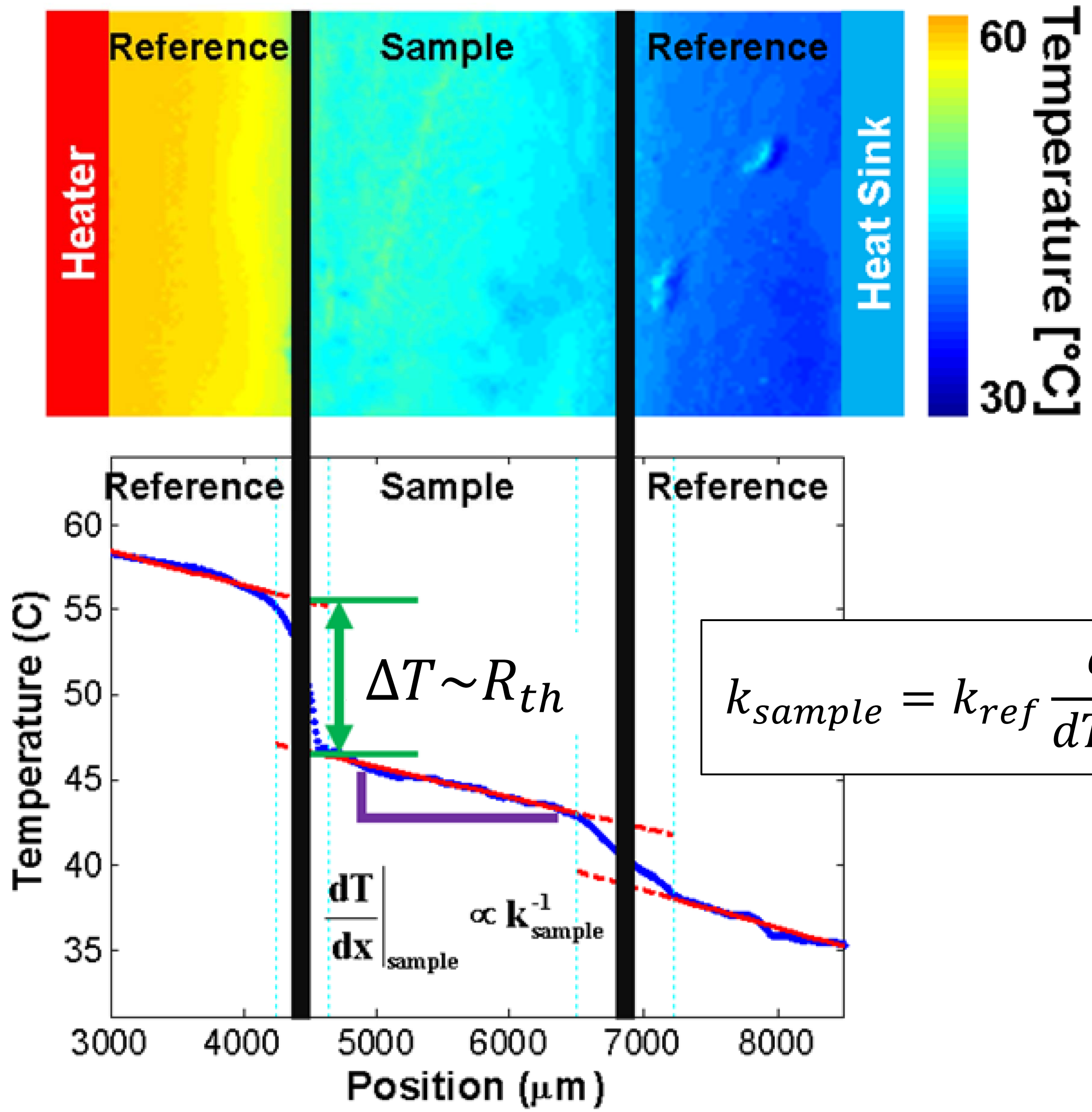

$$k_{sample} = k_{ref}\frac{dT/dx|_{ref}}{dT/dx|_{sample}}$$

Gaitonde, Nimmagadda, **Marconnet**: "Measurement of Thermal Conductance in Li-ion Batteries" *Journal of Power Sources* (2017).
DOI: 10.1016/j.jpowsour.2017.01.019

Barako, M.T., Gao, Y., Won, Y., **Marconnet, A.**, Asheghi, M., and Goodson, K.E., *IEEE Transactions on Components, Packaging and Manufacturing Technology* (2014).
DOI: 10.1109/TCPMT.2014.2369371

Separating Interfacial & Intrinsic Thermal Conductance

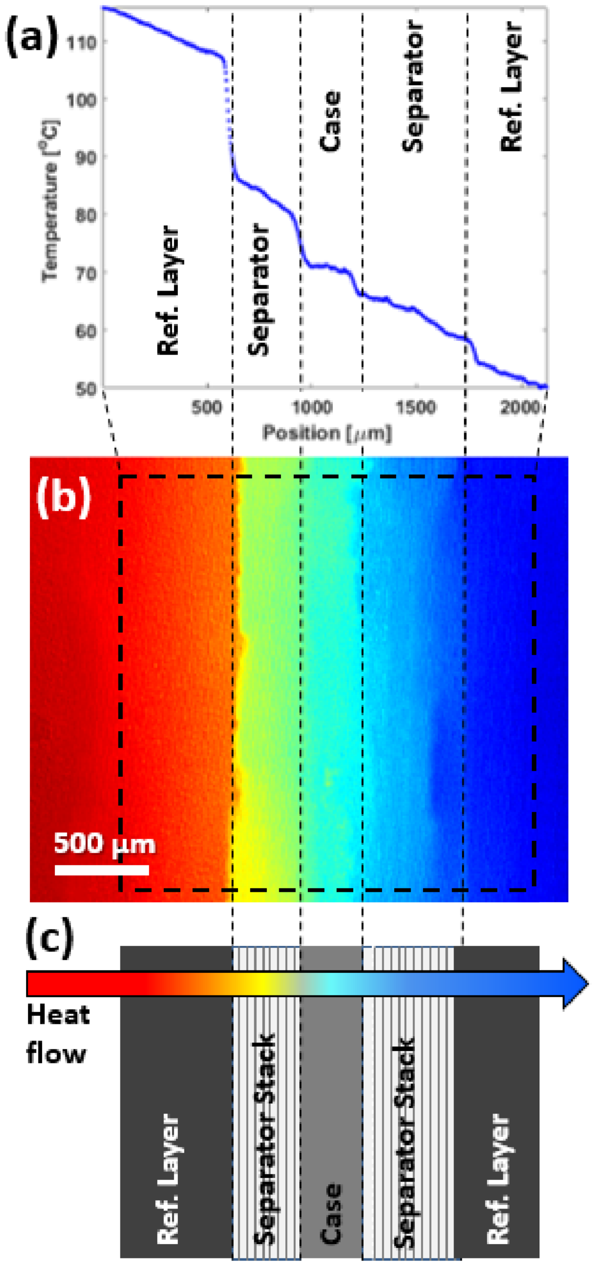

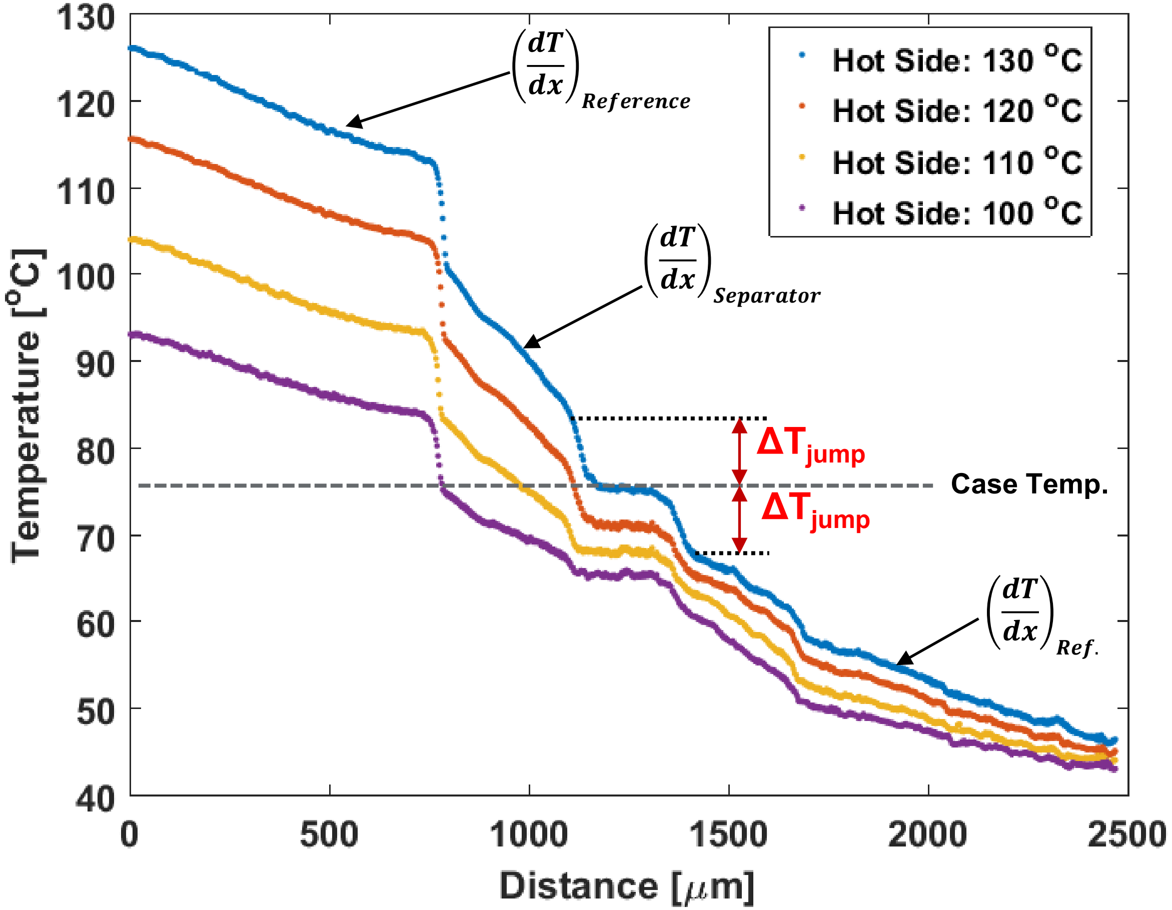

Temperature gradients across the sample stack, at four case temperatures

$$\textbf{Thermal Conductance: } G = \frac{q''}{\Delta T_{jump}}$$

Gaitonde, Nimmagadda, **Marconnet**: “Measurement of Thermal Conductance in Li-ion Batteries ” *Journal of Power Sources* (2017).

Interfacial Thermal Conductance

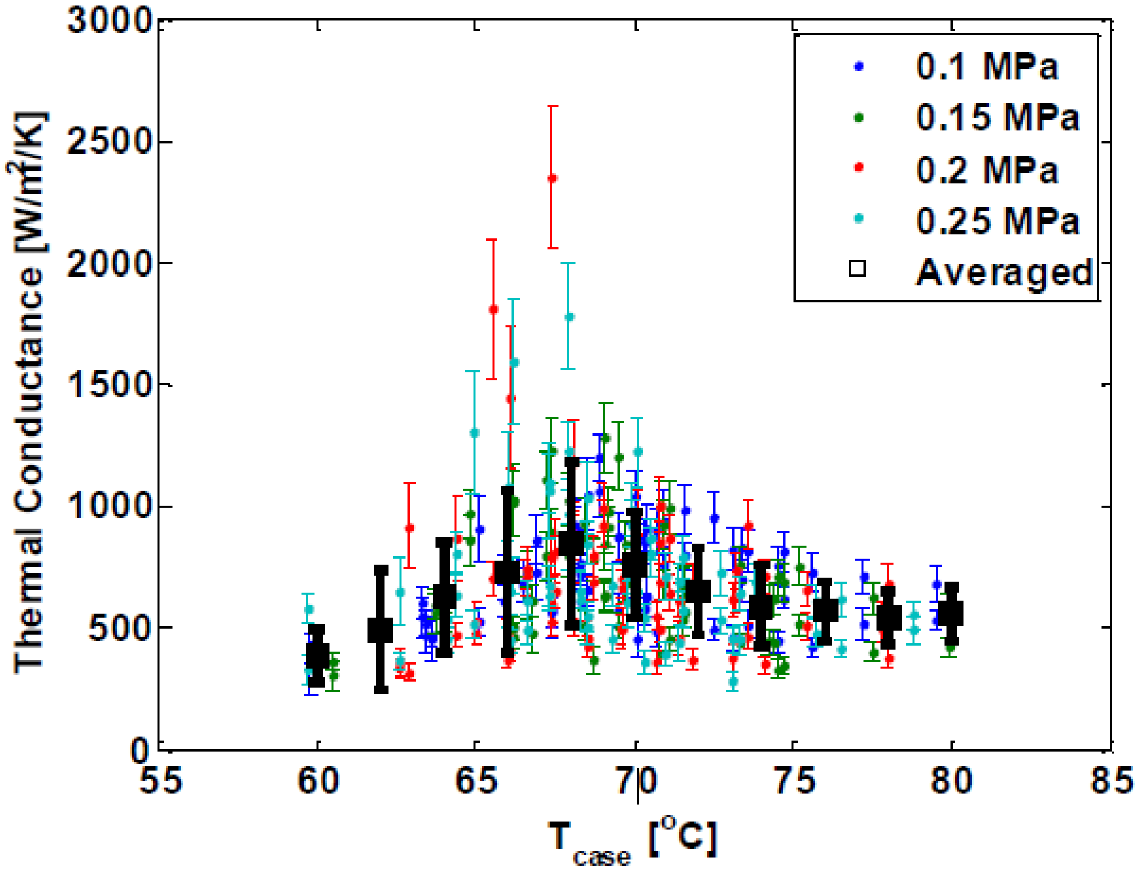

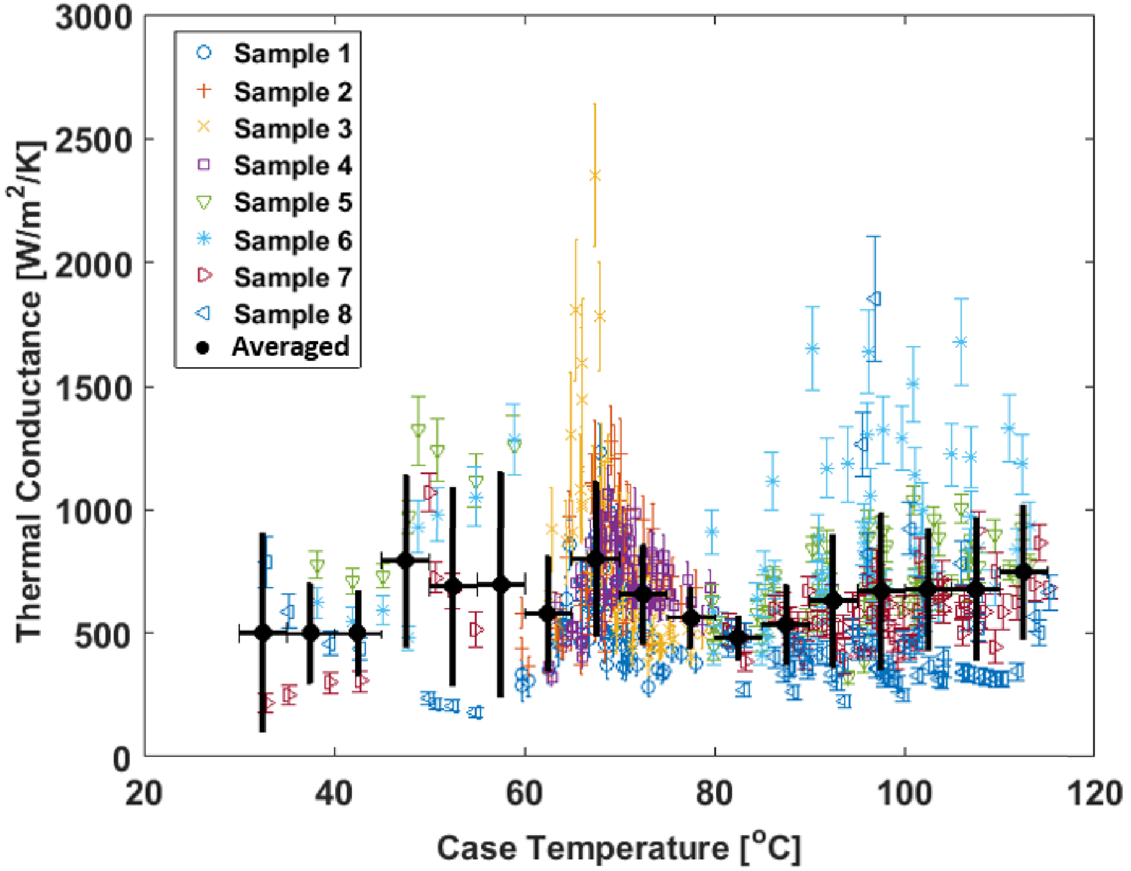

- **Interfaces Measured: 8**
- **Pressure Range: 0.1-0.25 MPa**
- **Case Temperatures: 30-120 °C**

Mean Thermal Conductance: 670 W/(m²K)
Standard Deviation: 275 W/(m²K)

Gaitonde, Nimmagadda, **Marconnet**: "Measurement of Thermal Conductance in Li-ion Batteries" *Journal of Power Sources* (2017).

Impact of Electrolyte

Sample	Component	*k* [W/(m K)]	
		Dry	Wet
Cathode (~15 layers)	Cu Foil double side coated by $LiMn_2O_4$	0.16 ± 0.06	0.45 ± 0.09
Anode (~15 layers)	AL Foil double side coated by CMS Graphite	0.57± 0.12	1.35 ± 0.49
Separator (~34 layers)	Ceramic Coated Membrane	0.10 ± 0.01	-
Stack (~12 layers)	Cathode +Separator + Anode	0.20 ± 0.04	0.44 ± 0.09

- Challenging to separate individual layer thermal properties from the interfacial effects, even with high resolution infrared microscopy
- Preliminary measurements show significant increase in effective thermal conductivity of cathode, anode, and stacks of the cathode-separator-anode with infiltration by a “mock electrolyte”

→Demonstrates importance of measuring samples with electrolyte

Heat Generation in Battery Cells

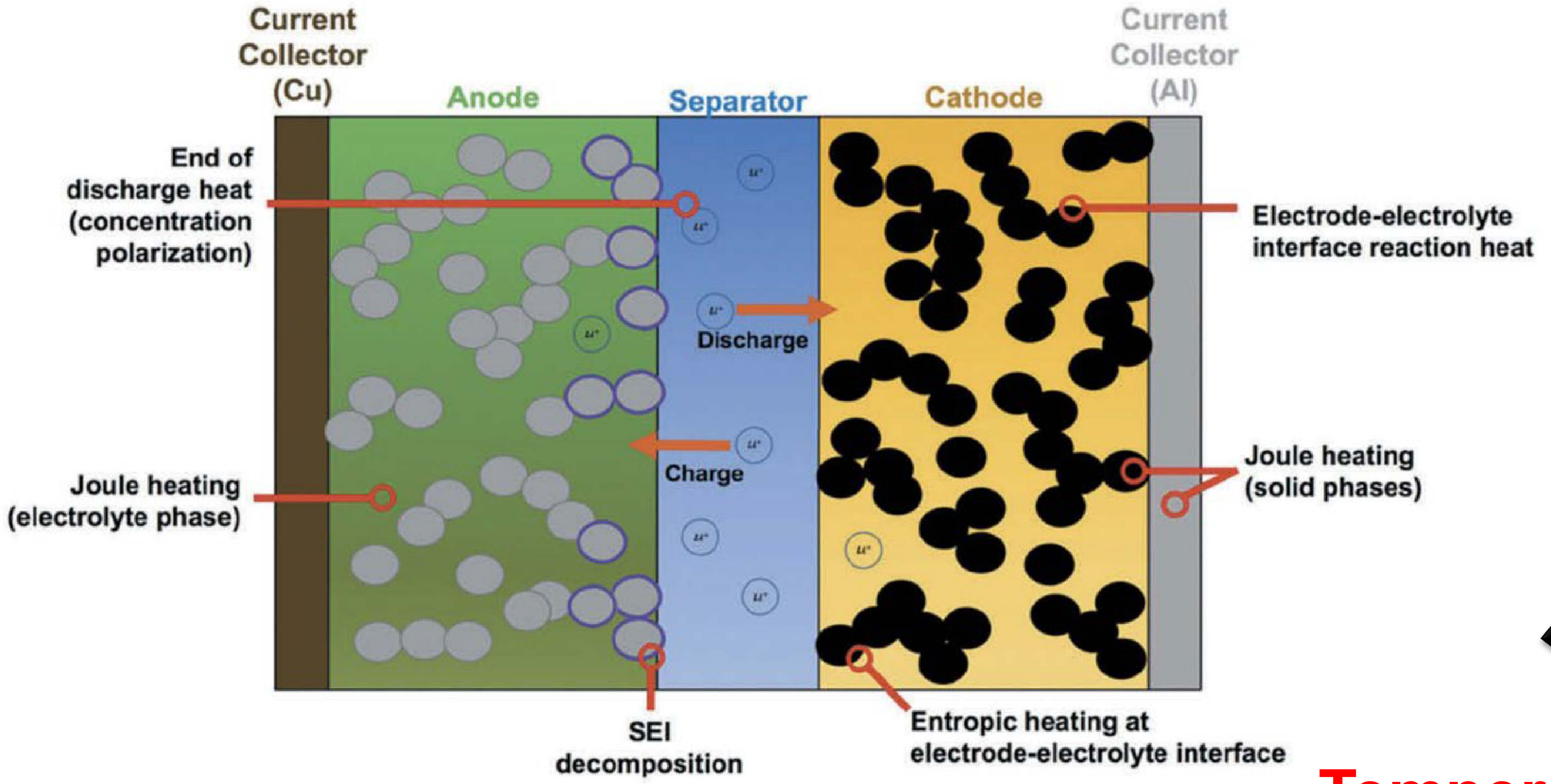

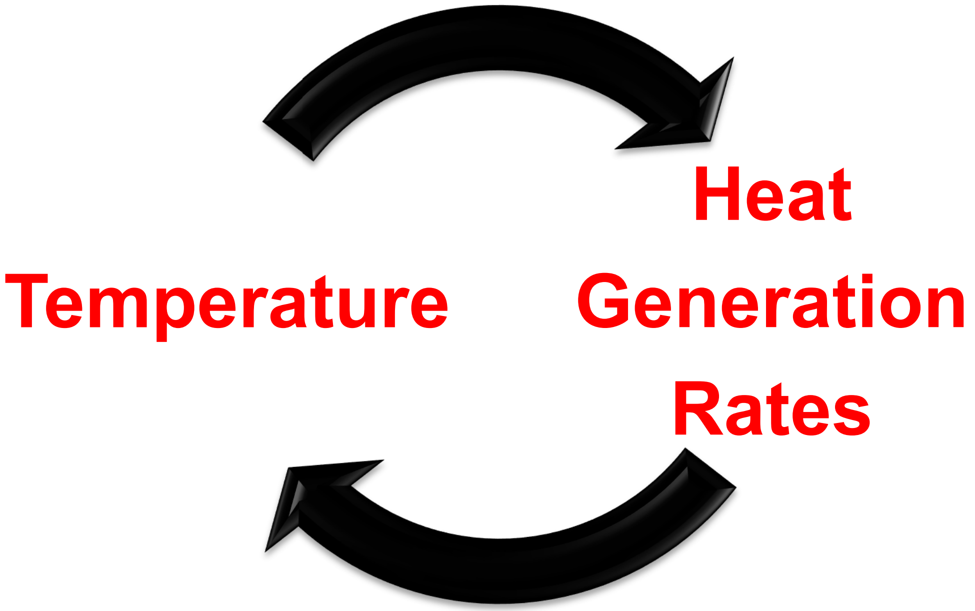

R. Kanatharaj & A. Marconnet, *Nanoscale and Microscale Thermophysical Enigneering*, vol. 23, no. 2, 2019.
DOI: 10.1080/15567265.2019.1572679

Ongoing Work: Local Temperatures & Heat Fluxes

- Open question: how do the evolving properties of the electrodes impact performance of battery cells?
- A student from KIT (Sven Stellmacher) visited Purdue completing their MS thesis on developing a tool to measure local temperatures during charging and discharging (with a goal to use this data to understand the local heat generation rates)
- To extract heat generation rates, we need the electrode in-plane conductivity

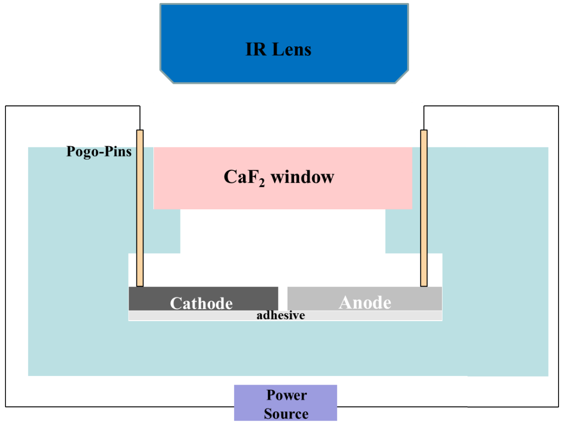

Preliminary Results

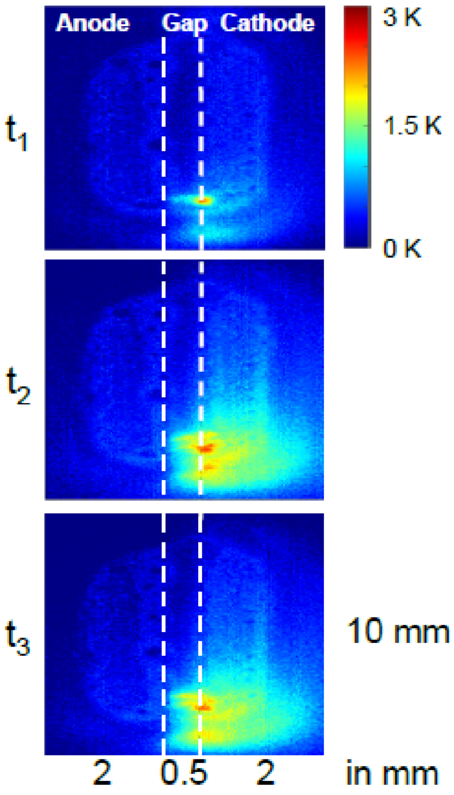

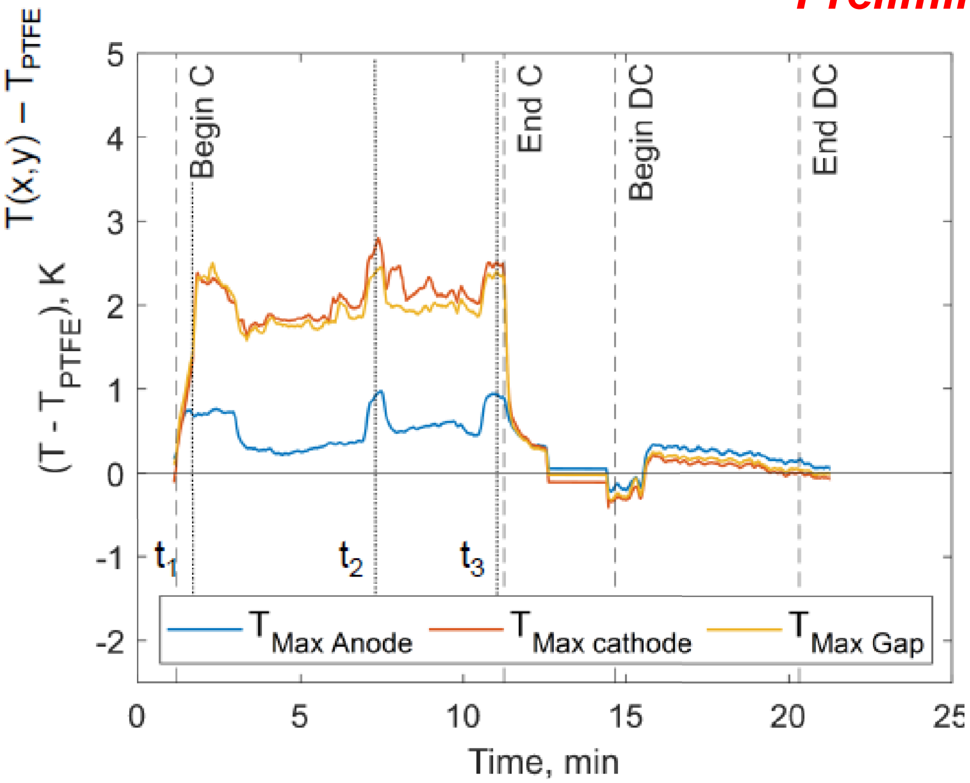

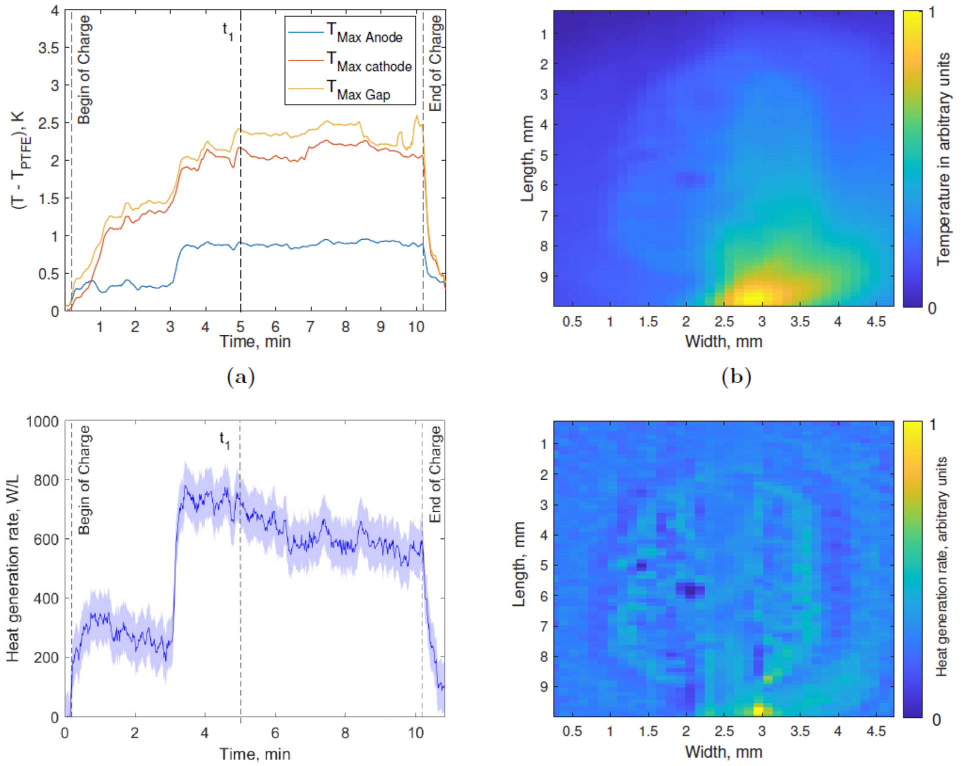

Measuring Temperatures during Charging

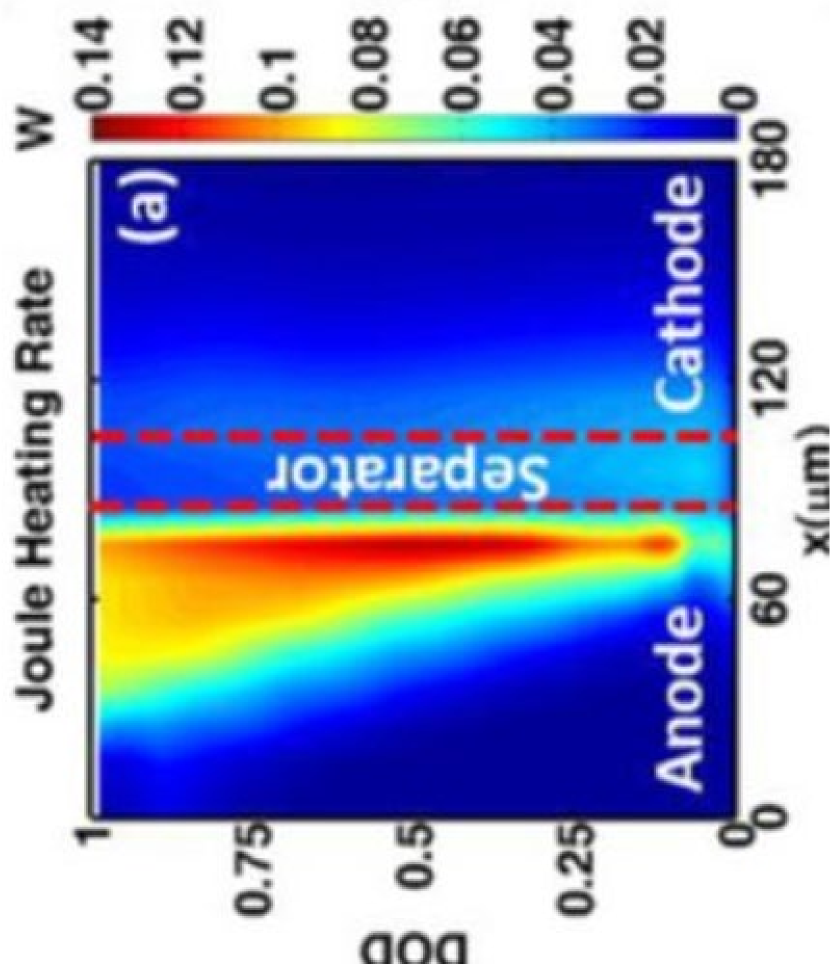

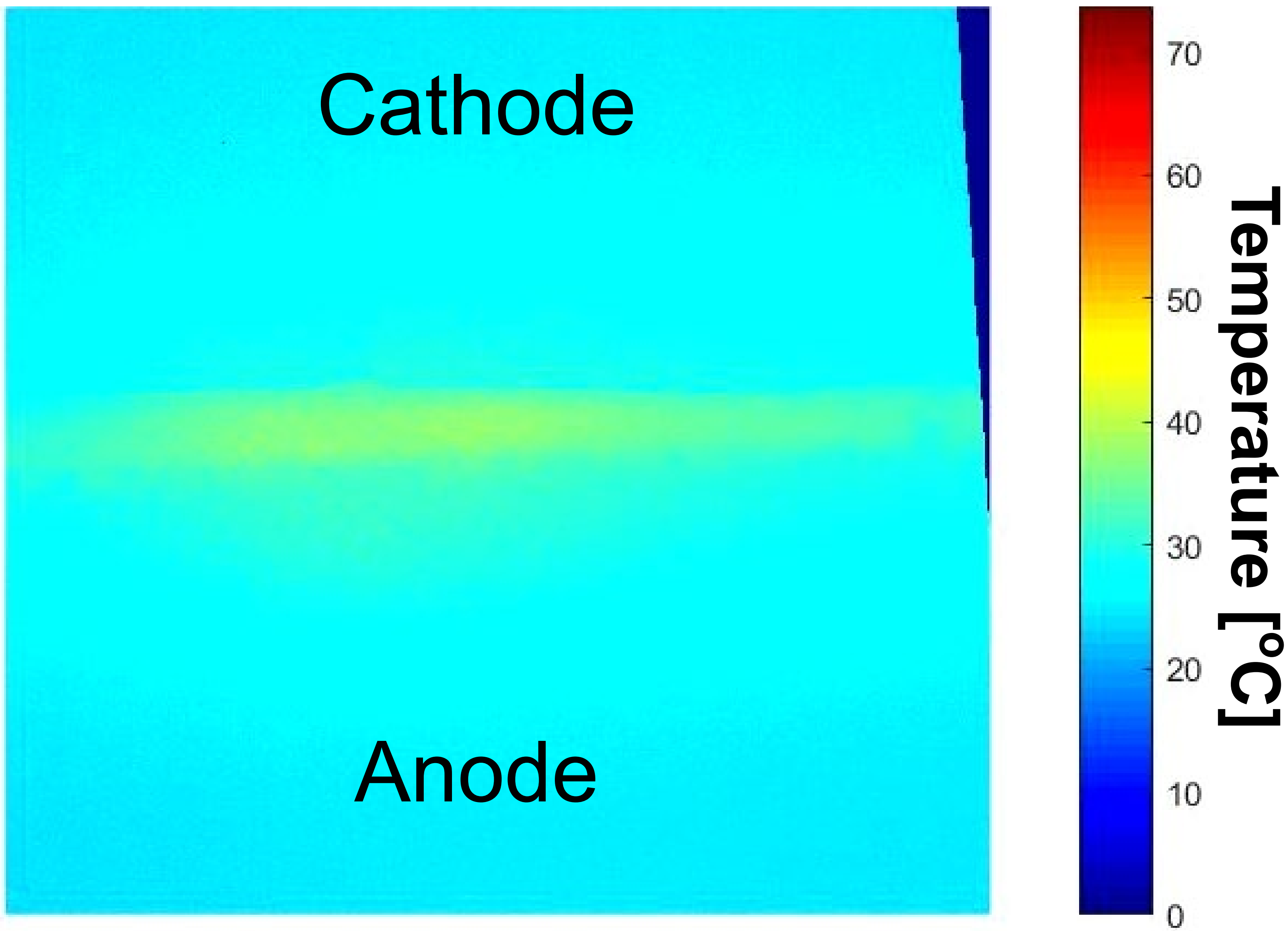

Chen *et* al. *J. Electrochem. Soc.* 2017 volume 164, issue 11, E3146-E3158. doi: 10.1149/2.0161711jes

Ongoing Work: Immersion Cooling & Multi-physics Modeling

GOALI Project with Valvoline and the Battery Innovation Center

Developing coupled thermal-electrochemical-mechanical-CFD models to predict cell temperature, electrochemical performance, and stresses

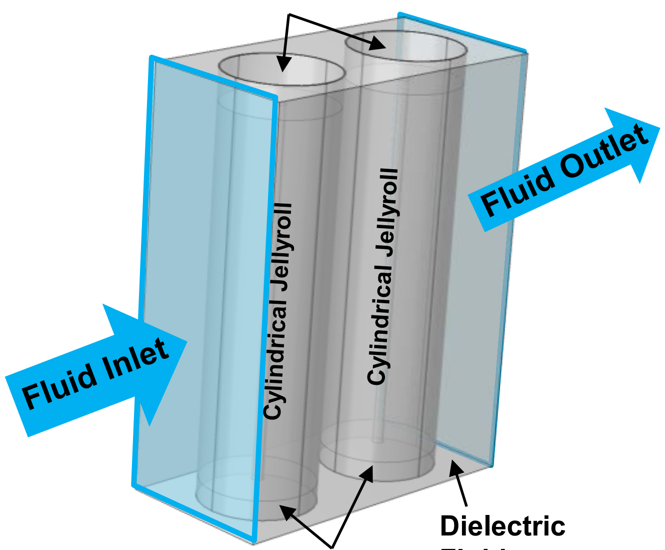

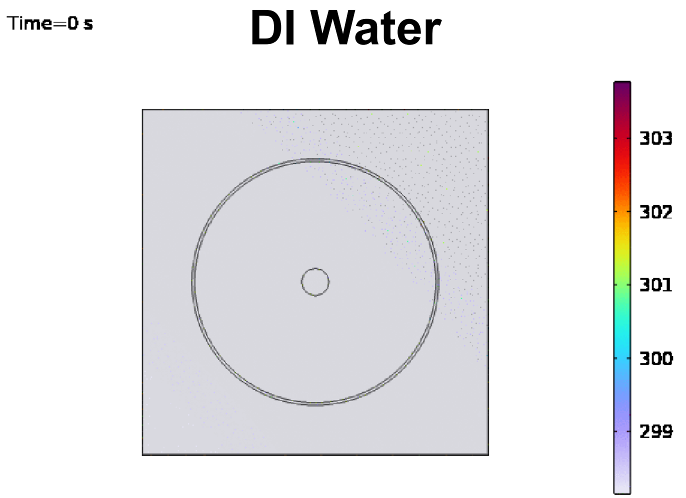

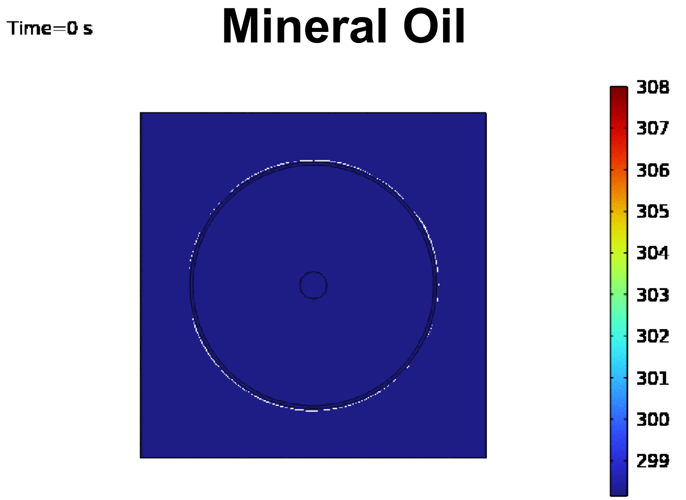

- Currently investigating impact of cooling solution on performance

Sensitivity to cooling fluid properties

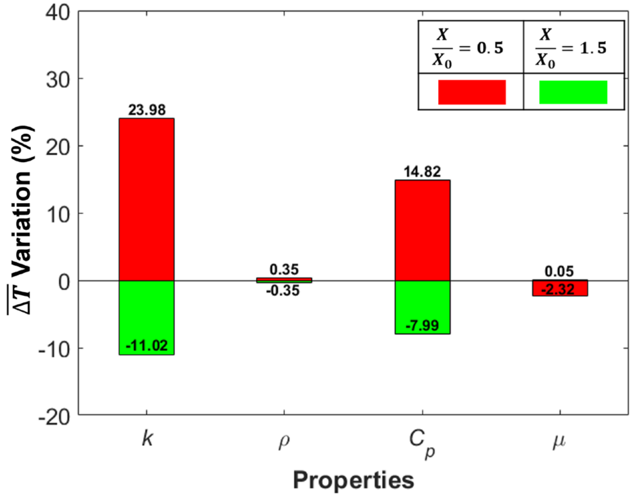

- Developing fast models leveraging quasi-analytical solutions to significantly reduce the computational cost without significantly sacrificing accuracy
- These fast models can be powerful tools for design and analysis of systems

Key Takeaway: Aging Reduces Thermal Transport Potentially Increasing Likelihood of Failure

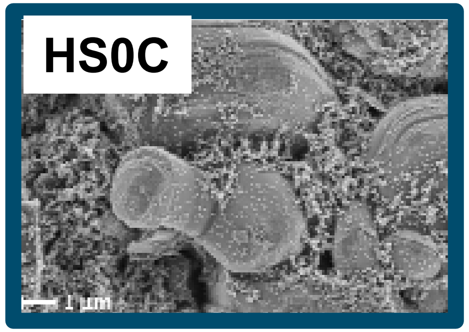

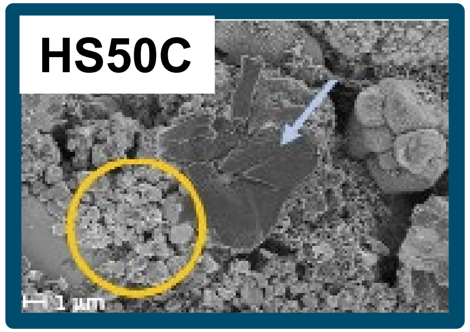

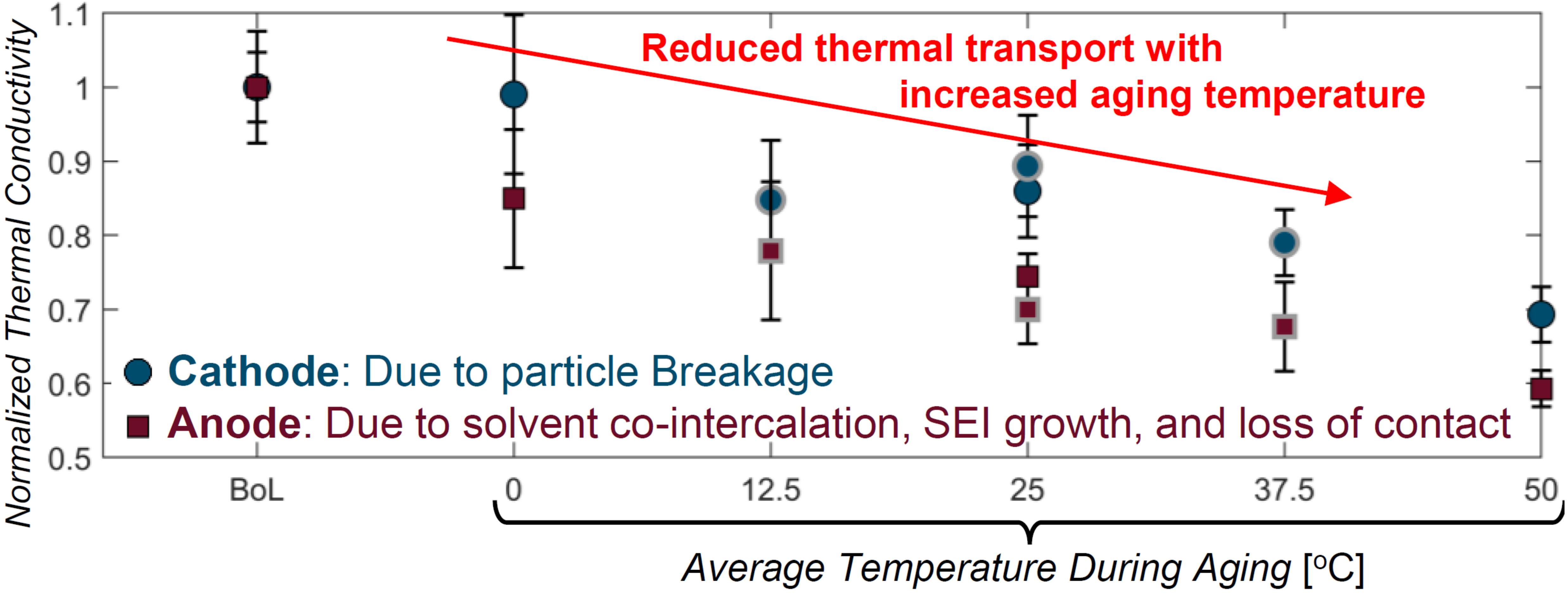

Questions & Comments

MTEC Lab @ Purdue

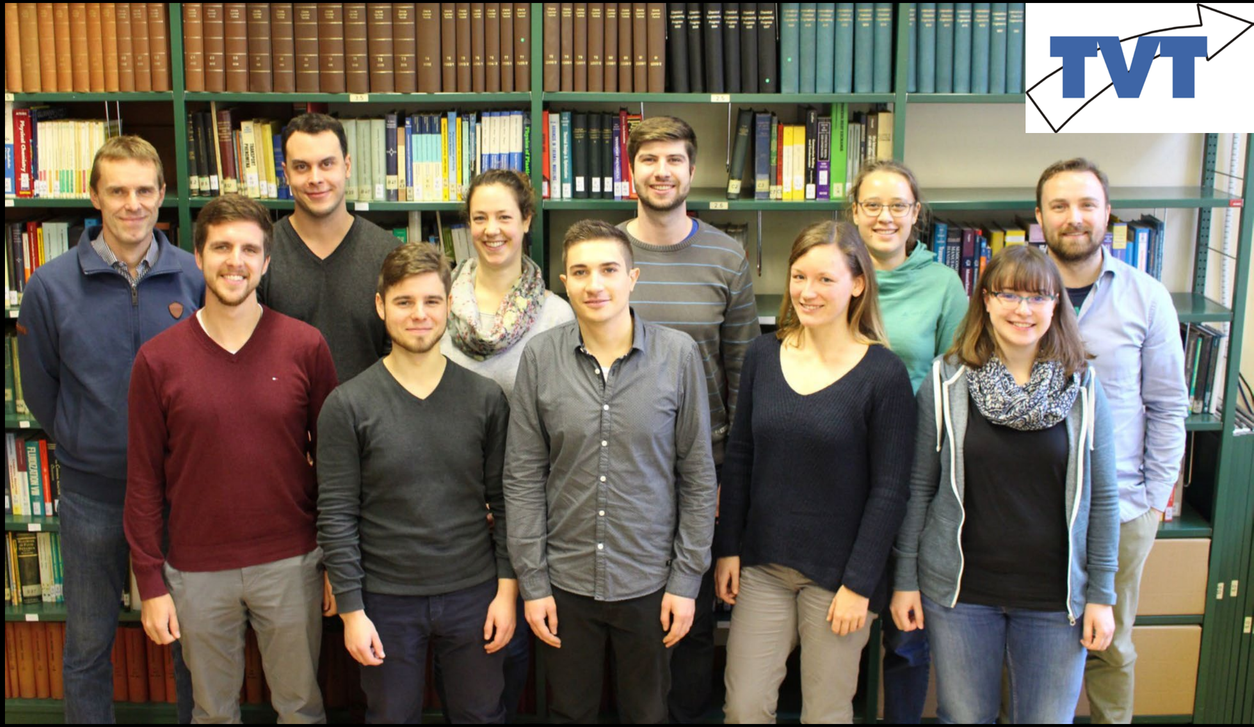

TVT @ KIT

Amy Marconnet
Mechanical Engineering
marconnet@purdue.edu
engineering.purdue.edu/MTEC

MTEC

PURDUE UNIVERSITY
Mechanical Engineering